



**HAL**  
open science

## Distribution and accumulation of metals and metalloids in planktonic food webs of the Mediterranean Sea (MERITE-HIPPOCAMPE campaign)

Sandrine Chifflet, Nicolas Briant, Javier Angel Tesán-Onrubia, Nouredine Zaaboub, Sirine Amri, Olivier Radakovitch, Daniela Bănaru, Marc Tedetti

### ► To cite this version:

Sandrine Chifflet, Nicolas Briant, Javier Angel Tesán-Onrubia, Nouredine Zaaboub, Sirine Amri, et al.. Distribution and accumulation of metals and metalloids in planktonic food webs of the Mediterranean Sea (MERITE-HIPPOCAMPE campaign). *Marine Pollution Bulletin*, 2023, *Marine Pollution Bulletin*, 186, pp.114384. 10.1016/j.marpolbul.2022.114384 . hal-03881849

**HAL Id: hal-03881849**

**<https://hal.science/hal-03881849>**

Submitted on 2 Dec 2022

**HAL** is a multi-disciplinary open access archive for the deposit and dissemination of scientific research documents, whether they are published or not. The documents may come from teaching and research institutions in France or abroad, or from public or private research centers.

L'archive ouverte pluridisciplinaire **HAL**, est destinée au dépôt et à la diffusion de documents scientifiques de niveau recherche, publiés ou non, émanant des établissements d'enseignement et de recherche français ou étrangers, des laboratoires publics ou privés.



Distributed under a Creative Commons Attribution - NonCommercial - NoDerivatives 4.0  
International License

1 **Distribution and accumulation of metals and metalloids in planktonic food webs of the**  
2 **Mediterranean Sea (MERITE-HIPPOCAMPE campaign)**

3

4 Sandrine Chifflet<sup>a\*</sup>, Nicolas Briant<sup>b</sup>, Javier Angel Tesán-Onrubia<sup>a</sup>, Noureddine Zaaboub<sup>c</sup>, Sirine Amri<sup>c</sup>,  
5 Olivier Radakovitch<sup>d,e</sup>, Daniela Bănaru<sup>a</sup>, Marc Tedetti<sup>a</sup>

6

7 <sup>a</sup> Aix Marseille Univ., Université de Toulon, CNRS, IRD, MIO UM 110, 13288 Marseille, France

8 <sup>b</sup> Ifremer, CCEM Contamination Chimique des Écosystèmes Marins, 44000 Nantes, France

9 <sup>c</sup> Institut National des Sciences et Technologies de la Mer (INSTM), 28 rue 2 mars 1934, Salammbô  
10 2025, Tunisia

11 <sup>d</sup> Aix Marseille Univ., CNRS, IRD, Collège de France, INRAE, CEREGE, 13545 Aix-en-Provence  
12 Cedex 4, France

13 <sup>e</sup> IRSN (Institut de Radioprotection et de Sécurité Nucléaire), PSE-ENV/SRTE/LRTA, Saint-Paul-Les-  
14 Durance, France

15

16 \* Corresponding author: sandrine.chifflet@mio.osupytheas.fr; Phone: + 33 4 86 09 05 32;

17 Fax: + 33 4 91 82 96 41

18

19 For submission to Marine Pollution Bulletin Special issue “*Plankton and Contaminants in the*  
20 *Mediterranean Sea: Biological pump and interactions from regional to global approaches*”

21 as a full-length research paper

22

23 Revised version

24 10 November 2022

25

26 **Abstract**

27 Particle-size classes (7 fractions from 0.8 to 2000  $\mu\text{m}$ ) were collected in the deep chlorophyll  
28 maximum along a Mediterranean transect including the northern coastal zone (bays of Toulon and  
29 Marseilles, France), the offshore zone (near the North Balearic Thermal Front), and the southern coastal  
30 zone (Gulf of Gabès, Tunisia). Concentrations of biotic metals and metalloids (As, Cd, Cr, Cu, Fe, Mn,  
31 Ni, Sb, V, Zn) bound to living or dead organisms and faecal pellets were assessed by phosphorus  
32 normalisation. Biotic metals and metalloids concentrations (except Cr, Mn, and V) were higher in the  
33 offshore zone than in the coastal zones. In addition, biotic Sb and V concentrations appeared to be  
34 affected by atmospheric deposition, and biotic Cr concentrations appeared to be affected by local  
35 anthropogenic inputs. Essential elements (Cd, Cu, Fe, Mn, Ni, V, Zn) were very likely controlled both  
36 by the metabolic activity of certain organisms (nanoeukaryotes, copepods) and trophic structure. In the  
37 northern coastal zone, biomagnification of essential elements was controlled by copepods activities. In  
38 the offshore zone, metals and metalloids were not biomagnified probably due to homeostasis regulatory  
39 processes in organisms. In the southern coastal zone, biomagnification of As, Cu, Cr, Sb could probably  
40 induce specific effects within the planktonic network.

41

42

43 **Keywords:** Metals and metalloids, planktonic food webs, Mediterranean Sea, Biomagnification,  
44 Contamination.

## 45 **Introduction**

46           The fate of metals and metalloids bound to particles in marine ecosystems has been widely  
47 studied since the 1950s, and research shows that these particle-bound metals and metalloids play an  
48 essential role in regulatory processes (Goldberg, 1954; Redfield, 1958; Turekian, 1977). Some of these  
49 particles come from natural sources due to soil alteration or volcanic emissions, while others come from  
50 anthropogenic sources due to mining, industrial, and urban activities (Nriagu and Pacyna, 1988; Burton  
51 and Statham, 1990; Donat and Bruland, 1995; Rauch, 2010). Over the past 30 years, several studies have  
52 shown that the distribution of metals and metalloids bound to particles in marine ecosystems was  
53 determined by complex biogeochemical cycles including both biotic and geochemical processes (Collier  
54 and Edmond, 1984; Bruland and Lohan, 2003; Sunda, 2012). Basically, biotic metals and metalloids  
55 (bM) in particles bind to organisms (living or dead) and faecal pellets *via* chemical mechanisms, whereas  
56 geogenic metals and metalloids in particles are primarily due to *in-situ* geochemical transformations or  
57 external lithogenic inputs.

58           Metals and metalloids can be classified as essential or non-essential elements for the marine  
59 food webs according to their role in biogeochemical cycles. Essential elements are necessary for  
60 physiological functioning and are used in various metabolic processes through energy or ion transfers  
61 (Morel et al., 2003). Non-essential elements have no specific biological relevance and can be toxic even  
62 at low concentrations. Although metals and metalloids can be passively introduced into marine food  
63 webs through porous membranes (skin and gills), the dominant pathway remains planktonic grazing  
64 (Whitfield, 2001; Chauvelon et al., 2019; Gao et al., 2021; Madgett et al., 2021). Depending on their  
65 concentrations, essential and non-essential elements can trigger toxic effects in whole organisms by  
66 altering respiration or digestion processes (Wang, 2002; Pérez and Beiras, 2010).

67           To assess potential environmental and human health risks, it is important to understand how  
68 planktonic species transfer metals and metalloids through marine food webs (Maxwell et al., 2013;  
69 Hazem et al., 2019; Sanganyado et al., 2021). In the field, the separation of metals and metalloids in  
70 particles bound to biotic (*i.e.*, organic matter from living and dead organisms and their faecal pellets)  
71 and geogenic (*i.e.*, minerals from natural and anthropogenic sources) components remains an operational  
72 challenge and requires ultra-clean techniques and environments to avoid contaminations (Cullen and

73 [Sherrell, 1999; Planquette and Sherrell, 2012](#)). Furthermore, efforts to quantify the bM fraction using  
74 modelling remain underdeveloped ([Ho et al., 2007, 2010; Liao et al., 2017](#)). Using *in vitro* experiments,  
75 [Ho et al. \(2003\)](#) proposed an extended Redfield formula ( $P_{1,000} Fe_{7.53} Mn_{3.84} Zn_{0.80} Cu_{0.38} Co_{0.19} Cd_{0.21}$ ) for  
76 eukaryotic phytoplankton species, but metals and metalloids contents relative to the biomass varied  
77 among species by a factor of about 20 (except for Cd, which varied by more than two orders of  
78 magnitude), this limiting attempt to generalise this model to ecological studies.

79 The transfer of metals and metalloids in marine food webs can be described using several  
80 metrics, such as the bioconcentration factor (BCF), bioaccumulation factor (BAF), biomagnification  
81 factor (BMF), or trophic magnification factor (TMF). However, these metrics are controlled by  
82 numerous parameters (species, size, metabolism, diet, community structure, environmental conditions,  
83 geographical location, *etc.*), which make ecotoxicological analysis an as-yet-unresolved challenge  
84 ([Burkhard et al., 2011; Cossa et al., 2022](#)).

85 The Mediterranean Sea is a semi-enclosed sea that represents ~ 0.7% of the total ocean surface  
86 (~ 0.25% in volume) and hosts 4%–18% of the world’s marine biodiversity ([Bianchi and Morri, 2000;](#)  
87 [UNEP/MAP-RAC-SPA, 2008](#)). Due to low nutrient concentrations and a phosphate deficit, the  
88 Mediterranean Sea is considered as oligotrophic ocean with low primary production ([Krom et al., 2010;](#)  
89 [Pujo-Pay et al., 2011; Tanhua et al., 2013](#)). In open waters, the concentration of chlorophyll *a* rarely  
90 exceeds 2–3 µg/L ([D’Ortenzio and d’Alcalà, 2009; The Mermex group, 2011; Marañón et al., 2021](#)).  
91 Planktonic food webs are structured by phytoplanktonic communities and carbon fluxes are controlled  
92 by a large microbial loop ([Uitz et al., 2006; Hunt et al., 2017; Mayot et al., 2017; Leblanc et al., 2018;](#)  
93 [Salhi et al., 2018; Ramírez-Romero et al., 2020](#)). However, the Mediterranean Sea is under both natural  
94 and anthropogenic pressure, because its waters are enriched by the deposition of atmospheric particles  
95 from large plumes of Saharan dust ([Guieu et al., 2002](#)) and by the increasingly intensive anthropogenic  
96 activities of its 22 bordering countries ([Grousset et al., 1995; Radakovich et al., 2008; Heimbürger et](#)  
97 [al., 2010; Chifflet et al., 2019; Migon et al., 2020](#)). In this context, plankton could be a key agent in the  
98 transfer of metals and metalloids in marine food webs ([Cossa and Coquery, 2005; Chauvelon et al.,](#)  
99 [2019](#)). To gain insight into this issue, the MERITE-HIPPOCAMPE campaign aims to evaluate the  
100 accumulation and transfer of metals and metalloids (and other inorganic and organic contaminants)

101 within planktonic food webs (bacterioplankton, phytoplankton, and zooplankton) in several  
102 geographical areas of the Mediterranean Sea. The objectives specifically addressed in this paper are: *i*  
103 to determine the concentrations of metals and metalloids in different plankton size-fractions (from  
104 bacteria to zooplankton), *ii* to assess the influence of plankton in the accumulation and transfer of metals  
105 and metalloids, and *iii* to establish links between geographical areas and metals and metalloids  
106 concentrations in plankton.

107

108

## 109 **1. Materials and methods**

### 110 *2.1 Study site*

111 The MERITE-HIPPOCAMPE campaign was carried out in the spring of 2019 along a North-  
112 South transect running between the French coast (Toulon and Marseilles, northwestern Mediterranean)  
113 and the Tunisian coast (Gulf of Gabès, southeastern Mediterranean) in two legs (Leg 1: St2, St3, St4,  
114 S10 and St11; Leg 2: St1, St9, St15, St17, St19) (Tedetti et al., 2022) (Fig. 1a, b; Table S1). Ten stations  
115 were chosen according to different criteria based on physical, biogeochemical and biological conditions  
116 and anthropogenic influences. St1–2 and St3–4, located respectively in the bays of Toulon and  
117 Marseilles, are strongly impacted by anthropogenic activities, and are ‘bloom’ or ‘intermittent bloom’  
118 areas according to D’Ortenzio and d’Alcalà (2009). St1 and St4 are the most ‘coastal’ stations whereas  
119 St2–3 are the most ‘offshore’ stations. Furthermore, St2–3 are located at the limit of the Ligurian  
120 ecoregion (Ayata et al., 2018). St9–10 are located near the northern zone of the North Balearic Front,  
121 and are ‘bloom’ and ‘intermittent bloom’ areas, respectively. The station St11, located in the Algerian  
122 ecoregion, is characterized by intense mesoscale eddies and is a ‘no bloom’ area according to the  
123 D’Ortenzio and d’Alcalà (2009) system. The station St15, located in the Gulf of Hammamet, is close to  
124 the Sicily Channel and exposed to influence from the Tunisian Atlantic current. It is a ‘no bloom’ area  
125 with a high density of small pelagic. St17 and St19 are located in the northern and southern parts of the  
126 Gulf of Gabès, respectively. The Gabès ecoregion (Ayata et al., 2018) is a hotspot of anthropogenic  
127 pressures and is characterized by shallow waters that are influenced by the Tunisian Atlantic current and  
128 by nutrient inputs from Saharan dust deposition or from sediment resuspension (Béjaoui et al., 2019).

129

## 130 2.2 Sampling and conditioning

131 Details of sampling procedures carried out as part of the MERITE-HIPPOCAMPE campaign  
132 can be found *infra* (Tedetti et al., 2022). The sampling strategy proposed a comprehensive end-to-end  
133 approach to study inorganic and organic contaminants in planktonic food webs (*i.e.* phyto-, zoo- and  
134 bacterio-plankton). Samples collected during this campaign had to be shared to carry out the numerous  
135 analyses planned. In order to collect enough plankton for all these analyses, we therefore focussed our  
136 strategy only on the deep chlorophyll maximum (DCM), during spring bloom (April to May), when  
137 maximum primary and secondary production occur (Lefevre et al., 1997; Marañón et al., 2021).

138 Briefly, at each station, various field operations were carried out at DCM to sample and sieve  
139 suspended particles (both biotic and geogenic) divided into 7 fractions (F1–7) ranging from 0.8 to 2000  
140  $\mu\text{m}$ . The smallest fractions (F1: 0.8–3  $\mu\text{m}$ , and F2: 3–20  $\mu\text{m}$ ) were sampled using a McLane pump  
141 (WTS6-142LV, 4–8 L/min) with mixed cellulose ester filters (MCE, Millipore) according to  
142 GEOTRACES recommendations (Cutter et al., 2017). The McLane pump was equipped with a 3-stage  
143 filter-holder and pre-cleaned filters (0.8  $\mu\text{m}$  MCE, 3  $\mu\text{m}$  MCE, 20  $\mu\text{m}$  nylon;  $\emptyset$  142 mm) (Bishop et al.,  
144 2012; Planquette and Sherrell, 2012). Pumping in the DCM lasted  $\sim$  50 min, thus filtering  $\sim$  240 L of  
145 seawater. On board, the residual seawater in the 3-stage filter holder was gently cleared by a peristaltic  
146 pump to ‘dry’ filters before storing them at  $-20$  °C. Three series of ‘blank filters’ were processed at the  
147 beginning, middle, and end of the campaign to assess possible contamination. These ‘blank filters’ were  
148 handled like all other filters without running McLane pumps.

149 Larger fractions ( $> 60$   $\mu\text{m}$ ) were sampled using a plankton net (Multinet, Hydro-Bios). During  
150 horizontal deployment of the Multinet in the DCM, ship speed was reduced to 2 knots for 30–100 min  
151 to allow a ‘gentle’ collection of particles (both biotic and geogenic). Once on the ship’s deck, the  
152 Multinet was rinsed with seawater and its contents (from five collectors) were transferred to pre-cleaned  
153 (HCl, 10%) 10-L perfluoroalkoxy (PFA) bottles. Then, working in a clean lab container, the particles  
154 (both biotic and geogenic) in the PFA bottle were fractionated using a nylon sieve column (60, 200, 500,  
155 1000, and 2000- $\mu\text{m}$  mesh sizes). The 5 fractions (F3: 60–200, F4: 200–500, F5: 500–1000, F6: 1000–  
156 2000, and F7  $> 2000$   $\mu\text{m}$ ) were sieved by ‘gentle’ filtration using a filtered seawater jet controlled by an

157 ASTI Teflon pump (Saint Gobain, model PFD2). Each fraction was transferred to pre-cleaned  
158 polycarbonate jars for storage (-20 °C) until analyses.

159

### 160 *2.3 Metals and metalloids analyses*

161 Sample processing was carried out according to GEOTRACES protocols (Bishop et al., 2012;  
162 Planquette and Sherrell, 2012; Cutter et al., 2017) in an ultra-clean trace metals laboratory (ISO 5), using  
163 high-purity acids (Fisher, Optima® grade or VWR, Normapur double-distilled acids) and MilliQ water.  
164 Before the MERITE-HIPPOCAMPE campaign, the MCE filters and their polyester sulfone storage  
165 boxes were pre-cleaned in 10% HCl (40 °C, overnight) and thoroughly rinsed with MilliQ water. Each  
166 MCE filter was slipped into a polyester sulfone box, dried under a laminar hood (ISO 1), labelled, pre-  
167 weighed, and stored in double-bagged polyethylene zip-lock bags. Likewise, polycarbonate jars  
168 equipped with screw caps (Nalgene) were pre-cleaned in 10% HCl (ultra-wave, 2 h) and thoroughly  
169 rinsed with MilliQ water, then the jars and caps were dried under a laminar hood (ISO 1), labelled, pre-  
170 weighed, and stored in double-bagged polyethylene zip-lock bags.

171 Back in the ultra-clean laboratory, the MCE filters (Ø142 mm) of the McLane pumps were  
172 freeze-dried, weighed, and sub-sampled using a stainless-steel cutter (Ø47 mm). Sub-samples were  
173 leached in PFA vials (Savillex) with 5 mL of a mixture of diluted acids (HF, 10%; HNO<sub>3</sub>, 50%), heated  
174 on a hot-block (120 °C, 5 h), evaporated to near-dryness, then re-dissolved in 3 mL HNO<sub>3</sub> (10%).  
175 Likewise, in-jar samples were freeze-dried and sub-samples (~200 mg dw) were leached in PFA vials  
176 (Savillex) with 5 mL of a mixture of pure acids (HF, 0.5 mL; HNO<sub>3</sub>, 4.5 mL), heated on a hot-block  
177 (120 °C, 24 h), evaporated to near-dryness, then re-dissolved in 3 mL HNO<sub>3</sub> (10%). Digested samples  
178 were then diluted using HNO<sub>3</sub> (2%) before running the metals and metalloids analyses. Metals and  
179 metalloids (As, Cd, Cr, Cu, Fe, Mn, Ni, Sb, Ti, V, Zn) were measured by inductively-coupled plasma  
180 mass spectrometry (Q-ICP-MS, Thermo-Scientific, iCAP-Q) using indium as an internal standard to  
181 correct for instrumental mass bias. The digestion procedure was assessed using a certified material for  
182 marine plankton (BCR 414, Commission of the European Communities). All elements were within the  
183 satisfactory recovery target of 100 ± 10% except for As (118%). Metals and metalloids concentrations  
184 in blank filters (0.8 and 3 µm MCE) were less than 1% of the mean metals and metalloids concentrations



185 measured in samples. The analytical detection limits were well below the sample concentrations. Further  
186 details are reported as supplementary information in [Tables S2 and S3](#).

187

#### 188 *2.4 Particulate organic phosphorus analyses*

189 The particulate organic phosphorus (POP) samples were oxidised by wet oxidation according to  
190 the procedure of [Raimbault et al. \(1999\)](#). Briefly, the oxidation of POP was carried out by the action of  
191 an oxidising reagent at 120 °C under alkaline buffered conditions. All chemicals used were of analytical  
192 grade quality. The oxidising reagent consisted of 30 g of borax ( $\text{Na}_2[\text{B}_4\text{O}_5(\text{OH})_4] \cdot 8\text{H}_2\text{O}$ ) and 15 g of  
193 potassium peroxydisulfate ( $\text{K}_2\text{S}_2\text{O}_8$ ) dissolved in 250 mL of MilliQ water. The digestion procedure was  
194 carried out in 50 mL pre-cleaned Pyrex bottles (Duran Schott). POP samples were placed in Pyrex  
195 bottles with 50 mL of MilliQ water and 5 mL of oxidising reagent and autoclaved at 120 °C for 30 min.  
196 Initial pH was 9.3 and pH remained alkaline (8.2) after digestion. After cooling at room temperature,  
197 the digestion mixture was directly pumped from the Pyrex bottle for colorimetric analysis using a  
198 Technicon AutoAnalyzer (Bran+Luebbe III) as described by [Aminot et al. \(2009\)](#).

199

#### 200 *2.5 Metals and metalloids in biotic component*

201 According to our sampling strategy, metals and metalloids concentrations measured in samples  
202 can be composed of both biotic and geogenic components. Geochemical studies often use elemental  
203 ratios as proxies to assess the origin or type of particles sampled. Since [Redfield's \(1958\)](#) pioneering  
204 studies dealing with phytoplanktonic communities, normalised ratios of particulate organic phosphorus  
205 (P-normalisation) have been widely used to assess biotic metals and metalloids bound to particles.  
206 Likewise, Ti is known to be a lithogenic element ([Ohnemus and Lam, 2015](#)) that is unaffected by  
207 scavenging, biological uptake or particulate recycling ([Dammshäuser et al., 2013](#)) and can thus be used  
208 in normalisation ratios to assess geogenic metals and metalloids bound to particles ([Lemaitre et al.,](#)  
209 [2020](#)). Metals and metalloids concentrations in samples can therefore be expressed using the mass  
210 balance formula ([Ho et al., 2007](#); [Liao et al., 2017](#)):

211

$$[M]_{\text{sample}} = a \cdot [Ti]_a + b \cdot [POP]_b \quad (1)$$

212 where a is the Ti-normalised elemental ratio in the geogenic component, b is the P-normalised elemental  
213 ratio in the biotic component,  $[M]_{sample}$  is the concentration of the element in the sample,  $[Ti]_a$  is the  
214 concentration of Ti in the geogenic component, and  $[POP]_b$  is the concentration of particulate organic  
215 phosphorus (POP) in the biotic component. Assuming that POP and Ti in samples are mainly due to the  
216 biotic and geogenic components, respectively ( $[POP]_{sample} \equiv [POP]_b$ ;  $[Ti]_{sample} \equiv [Ti]_a$ ), we can turn the  
217 mass balance formula into first-order equation 2:

$$218 \quad \frac{[M]_{sample}}{[Ti]_{sample}} \equiv S \cdot \frac{[POP]_{sample}}{[Ti]_{sample}} + C \quad (2)$$

219 where S is the slope of the regression line between M/Ti and POP/Ti in the sample, and C is a constant  
220 value. Following this basic model, metals and metalloids concentrations in the biotic component (bM  
221 concentrations) were evaluated from the slopes of the regression lines between M/Ti and POP/Ti in the  
222 sample. The slope S was calculated for each station and for each element using the 7 particle-size classes  
223 from F1 to F7 (see [Appendix 1 for supplementary information](#)). Since the purpose of this study was to  
224 evaluate transfers and accumulations of metals and metalloids in planktonic food webs  
225 (bacterioplankton, phytoplankton and zooplankton), we focus here only on the bM component, as the  
226 geogenic component is not directly involved in these mechanisms.

227

## 228 *2.6 Trophic magnification factor*

229 The trophic magnification factor (TMF) represents the diet-weighted mean transfer of an  
230 element throughout food webs ([Burkhard et al., 2011](#)). In practice, TMF is most often derived from the  
231 slope of the regression of a log-transformed elemental against its corresponding trophic level (TL), and  
232 the N isotope ( $\delta^{15}N$ ) is used as a proxy to assess the relative trophic position of an organism in food  
233 webs ([Borgå et al., 2012](#); [Kidd et al., 2018](#); [Tesán-Onrubia et al., 2022](#)).

$$234 \quad \text{Log}_{10}(bM) = S \cdot (TL) + C \quad (3)$$

$$235 \quad TMF = 10^S \quad (4)$$

236 where bM is biotic elemental concentration, S is the slope of the linear equation 3, and TL is the trophic  
237 level corresponding to the sample. Specific TMFs (equation 4) were calculated for each geographical  
238 area from their respective data (see [Appendix 2 for supplementary information](#)). A TMF > 1 indicates

239 accumulation of an elemental in food webs, while a TMF < 1 suggests dilution of an elemental in high  
240 trophic levels. TMF can be influenced by many factors, such as physiology, migration and lifetime of  
241 the species, spatio-temporal variability of the elements, metabolic functioning, *etc.*

242

## 243 *2.7 Statistical analyses*

244 All statistical analyses were performed using Xlstat software package version 2019.1.1  
245 (Addinsoft 2020, Boston, USA, <https://www.xlstat.com>). First, Shapiro-Wilks tests were used to check  
246 the normality of variances. Next, parametric tests (ANOVA test) or non-parametric tests (Kruskal-  
247 Wallis test) were used to examine potential differences between data. Box plot were used to show  
248 variations of bM concentrations in size fractions per geographical areas. Parametric tests (Student t-test)  
249 or non-parametric tests (Mann-Whitney-Wilcoxon test) were used to examine the effect of geography  
250 on bM concentrations.

251

## 252 **2. Results and discussion**

### 253 *3.1 Spatial variability and stoichiometry of metals and metalloids in the biotic compartment*

254 Due to the high spatio-temporal variability between stations (Tedetti et al., 2022), bM  
255 concentrations were grouped by broad geographical areas, *i.e.* the northern coastal zone (4 stations, St1  
256 to St4), the offshore zone (3 stations, St9 to St11) and the southern coastal zone (3 stations, St15, St17,  
257 and St19) based on the hydrological context (Boudriga et al., 2022). Table 1 summarises bM  
258 concentration ranges (mean ± standard deviation, min and max) in all fractions (F1–7) per element and  
259 geographical area, and Table S4 details the results per element, station, and fraction. Variations in bM  
260 concentrations were examined according to geographical areas and statistical tests (ANOVA or KW  
261 tests,  $p < 0.05$ ) (Table S5). Most metals and metalloids were significantly found at higher mean bM  
262 concentrations in the offshore zone, except for Cr and V that had significantly higher mean bM  
263 concentrations in the northern coastal zone and Mn that displayed significantly higher mean bM  
264 concentration in the southern coastal zone. Large fluctuations were observed in bM concentrations, as  
265 indicated by the high coefficients of variation (CV), with no clear trends emerging, either by element or  
266 by geographical area (Table 1). For example, highest bM variations were found for V in the northern

267 coastal zone (CV = 183%), for Sb in the offshore zone (CV = 166%) and for Mn in the southern coastal  
268 zone (CV = 159%). Conversely, lowest CV were found for Ni in the northern coastal zone (CV = 45%),  
269 for Cu in the offshore zone (CV = 40%) and for Cd in the southern coastal zone (CV = 48%). In the  
270 Mediterranean Sea, data of bM were sparse or incomplete and varied according to sampling strategy  
271 (sampling depth, spatio-temporal characteristics and, plankton size fractions), making comparisons a  
272 risky exercise. However, our results shared strong overlaps with metals and metalloids concentrations  
273 measured in zooplankton collected offshore of the Italian coasts in the cyclonic current of the Ligurian  
274 Sea (Battuello et al., 2016), and were less than or equal to the metals and metalloids concentrations of  
275 suspended particles collected at the DCM in the Gulf of Lions (Chouvelon et al., 2019).

276 Mean bM/POP ratios were calculated to present metals and metalloids stoichiometry per  
277 fractions (F1–7) and per geographical area (Table 2; Table S6 for bM/POP ratios detailed per station).  
278 Differences between geographical areas were tested using statistical analyses (ANOVA or KW tests,  $p$   
279  $< 0.05$ ). Significant differences in bM/POP ratios were found for all metals and metalloids except Fe, V  
280 and Zn (Table S7). These results suggest that metals and metalloids (except Fe, V and Zn) influence the  
281 physiology and ecology of planktonic food webs (0.8–2000  $\mu\text{m}$ ) in the Mediterranean Sea. Indeed,  
282 metals and metalloids concentrations in marine food webs depend on the physiological accumulation  
283 strategies of pelagic species and may vary between different taxonomic groups in the same ecosystem  
284 (Ho et al., 2003; Quigg et al., 2003; Twining and Fisher, 2004; Morel, 2008). For example, in small  
285 planktonic food webs, metals and metalloids accumulation is particularly efficient when copepods feed  
286 on protozoa rather than phytoplankton (Twining and Fisher, 2004). By effectively controlling the efflux  
287 of metals and metalloids, copepods play a key role in metals and metalloids distribution within  
288 planktonic food webs (Wang et al., 2002; Battuello et al., 2017). Our results showed that mean bM/POP  
289 ratios varied in the same decreasing order  $\text{Fe} > \text{Zn} > \text{As} \sim \text{Cr} \sim \text{Cu} \sim \text{Mn} \sim \text{V} > \text{Ni} \sim \text{Sb} > \text{Cd}$  in the three  
290 geographical areas. These findings are in good agreement with Twining and Baines (2013) who  
291 generalised phytoplanktonic M/P ratios from geochemical data as follows:  $\text{Fe} \sim \text{Zn} > \text{Mn} \sim \text{Ni} \sim \text{Cu} \gg$   
292 Cd.

293

294 *3.2 Biotic metals and metalloids distribution in planktonic food webs*

295 Fig. 2 and 3 show boxplots representing the distribution of 7 major essential elements (Cd, Cu,  
296 Fe, Mn, Ni, V, Zn) and 3 non-essential elements (As, Cr, Sb) per fractions (F1–7) and geographical area  
297 (northern coastal zone, offshore zone, and southern coastal zone), respectively. Essential elements are  
298 known to control plankton physiology (Whitfield, 2001; Morel et al., 2003; Twining and Baines, 2013)  
299 but trophic relationships are extremely complex, and the distribution of bM in planktonic food webs can  
300 be influenced by many factors, such as community structure, environmental conditions, and spatio-  
301 temporal sampling plan (Battuello et al., 2016). Differences in bM concentrations between geographical  
302 areas were assessed using statistical tests (Student or Mann-Whitney-Wilcoxon tests,  $p < 0.05$ ) (Table  
303 S8).

304 The planktonic community related to the MERITE-HIPPOCAMPE campaign is extensively  
305 described in Boudriga et al. (2022) and Fierro-González et al. (2022) as companion papers. Briefly, the  
306 smallest phytoplanktonic fractions were mainly composed of picoeukaryotes for F1 and nanoeukaryotes  
307 for F2, while the largest zooplanktonic fractions were composed of nauplii and copepods for F3,  
308 copepods of increasing size for F4 and F5, large copepods and small crustaceans for F6, and crustaceans  
309 and gelatinous organisms for F7.

310

### 311 3.21 Essential elements

312 The concentration of essential elements followed three different patterns of distribution  
313 depending on the geographical area (Fig. 2). In the northern coastal zone, bM concentrations showed a  
314 bell-shaped distribution with a maximum in the F4–5 range (mainly composed of copepods). In the  
315 offshore zone, bM concentrations showed a flat-shaped distribution with a maximum in the F2–5 range  
316 (from nanoeukaryotes to copepods). In contrast, in the southern coastal zone, the bM concentrations  
317 showed increase from F1 to F5 (F6 and F7 were not available due to a lack of particles  $> 1000 \mu\text{m}$ ).

318 Biotic Cd concentrations presented two-modal distributions in the three geographical areas, with  
319 two maxima ( $\sim 1 \mu\text{g/g}$ ) in the F1 and F4 fractions composed of picoeukaryotes and small copepods,  
320 respectively. No significant differences were found between the three geographical areas and bCd  
321 concentrations. Cd is considered an essential element as it influences both growth and structure of  
322 communities (Lee et al., 1995; Lane and Morel, 2000; Xu et al., 2008). The biochemical activity of Cd

323 could be due to a strong reactivity with polyphosphate sites together with a rapid uptake into the cell *via*  
324 the Zn transport system (Whitfield, 2001). Cd speciation is planktonic species-dependent. For example,  
325 in small plankton sizes, Cd assimilation is particularly efficient when copepods feed on protozoa rather  
326 than phytoplankton (Twining and Fisher, 2004). In higher plankton sizes, cephalopods and crustaceans  
327 accumulate more Cd than other planktonic species (Liu et al., 2019). Therefore, the two-modal  
328 distribution of bCd in planktonic food webs might reveal prey-predator relationship between  
329 picoeukaryotes and small copepods in the three geographical areas. Unfortunately, due to the relatively  
330 small dataset, this suggestion needs further investigation.

331 Maximum bCu concentrations ( $\sim 7 \mu\text{g/g}$ ) were found in the F5 fractions in the three  
332 geographical areas. No significant differences in bCu concentrations were found between the northern  
333 and southern coastal zones, but significant differences in bCu concentrations were found between the  
334 northern coastal zone and offshore zone and between the offshore zone and the southern coastal zone.  
335 The Mediterranean Sea is under strong anthropogenic pressure, both on a large scale by atmospheric  
336 deposition and more locally near coastal zones by urban/industrial inputs (Guieu et al., 2010;  
337 Heimbürger et al., 2010; Chifflet et al., 2019; Gargouri et al., 2021). Surface waters can either be  
338 depleted or enriched in Cu according to the seasonal intensity of phytoplankton activity (Heimbürger et  
339 al., 2011; Migon et al., 2020). In the western Mediterranean Sea, the high Cu concentrations in  
340 atmospheric deposition, are known to decrease the phytoplanktonic biomass (Jordi et al., 2012). Cu is  
341 an essential element for organisms but can have a negative effect in eukaryote communities when free  
342 Cu exceeds 10 pM (Sunda and Huntsman, 1995). Above this threshold, primary producers (bacteria,  
343 prokaryotes and eukaryotes) exude organic ligands that strongly complex free Cu, rendering it non-  
344 bioavailable (Moffett and Brand, 1996; Croot et al., 2000; Muller et al., 2005). The two-modal curve in  
345 the offshore and northern coastal zones could indicate an active homeostasis regulation of Cu within the  
346 smallest size fractions (F1–2). Furthermore, copepods (abundant in F5) have a high requirement for Cu  
347 because they used this metal in complexation reactions with amino acids or proteins such as glutathione  
348 or metallothionein, respectively (Roesijadi and Robinson, 1994; Rainbow, 2007; Barka et al., 2010; Tlili  
349 et al., 2016). Isotopes can also be used as proxies of biogeochemical processes (Takano et al., 2014;  
350 Moynier et al., 2017). In a companion study (Chifflet et al., 2022), statistical analyses (non-parametric

351 Spearman tests) were used to assess relationships between Cu isotopic compositions and copepods. In  
352 the northern coastal zone and offshore zone, Spearman's correlation coefficients were weak ( $r = 0.14$   
353 and  $-0.10$ , respectively) whereas in the southern coastal zone, the Spearman's correlation coefficient  
354 was significantly higher ( $r = -0.94$ ,  $p < 0.05$ ). This result suggests that Cu negatively impact copepods'  
355 activities in the southern coastal zone. Due to the large anthropogenic inputs in this area, effects of Cu  
356 on planktonic food webs should be further investigated.

357 Biotic Fe presented the same distribution patterns as bCu in the three geographic areas with the  
358 highest bFe concentrations for F5 ( $\sim 250 \mu\text{g/g}$ ) in the northern coastal zone, for F2 and F6 ( $\sim 550 \mu\text{g/g}$ )  
359 in the offshore zone, and for F5 ( $\sim 350 \mu\text{g/g}$ ) in the southern coastal zone. No significant differences in  
360 bFe concentrations were found between the northern and southern coastal zones, but significant  
361 differences in bFe concentrations were found between the northern coastal zone and offshore zone and  
362 between the offshore zone and the southern coastal zone. This essential element is well-known to play  
363 a key role in biochemical electron transfer processes by increasing the amount of Fe in phytoplankton  
364 and heterotrophic bacteria (Whitfield, 2001). The Mediterranean Sea is subject to recurrent natural and  
365 anthropogenic dust deposition events leading to surface waters generally enriched in Fe so that the  
366 phytoplankton growth is not limited by Fe (Chester et al., 1996; Guieu et al., 1997; Heimbürger et al.,  
367 2011; Migon et al., 2020). Based on these considerations, our results suggest the absence of Fe limitation  
368 in Mediterranean Sea.

369 Biotic Mn was the only essential element that showed a bell-shaped distribution in the southern  
370 coastal zone, with a maximum bMn concentration in F2 ( $\sim 30 \mu\text{g/g}$ ). No significant differences were  
371 found between the three geographical areas and bMn concentrations. In a previous study, Mn was found  
372 to bioaccumulate significantly in the smallest marine species (Srichandan et al., 2016) and same Mn  
373 concentrations were found in plankton ( $0.7\text{--}20 \mu\text{m}$ ) from the Gulf of Guinea (Chevrollier et al., 2022).  
374 Furthermore, feeding behaviour could influence the Mn concentrations in larger plankton ( $> 300 \mu\text{m}$ )  
375 (Battuello et al., 2017). High bMn concentrations in F2 (nanoeukaryotes) might be easily assimilated by  
376 larger plankton (F3–7) and partially excreted *via* dietary pathway. The decrease of bMn concentrations  
377 in larger plankton size might be also explained by a 'bio-dilution' effect due to variations in the size of



378 organisms. Due to numerous mechanisms impacting Mn transfer, controlled laboratory experiments are  
379 needed to elucidate the role of plankton and environmental conditions in the bM distribution.

380 Biotic Ni concentrations showed higher variabilities in the offshore and the southern coastal  
381 zones (from ~ 1.5 to 3.5  $\mu\text{g/g}$  and from ~ 1 to 3.5  $\mu\text{g/g}$ , respectively) than in the northern coastal zone  
382 (from ~ 1 to 1.5  $\mu\text{g/g}$ ). No significant differences in bNi concentrations were found between the northern  
383 and southern coastal zones, but significant differences in bNi concentrations were found between the  
384 northern coastal zone and offshore zone and between the offshore zone and the southern coastal zone.  
385 Ni is an essential element for the assimilation of urea, which can be a significant source of nitrogen in  
386 biological processes (Whitfield, 2001; Morel et al., 2003). An increase in Ni uptake rates can be  
387 observed when phytoplankton (*Synechococcus*, *Prochlorococcus*) consume nitrate rather than  
388 ammonium (Dupont et al., 2008). Ni uptake by copepods depends on the exposure routes, and  
389 homeostasis regulation are species dependent (Kadiene et al., 2009). These authors showed that in  
390 copepods (*Pseudodiaptomus annandalei* and *Eurytemora affinis*), Ni uptake is substantially higher when  
391 this metal is absorbed directly from dissolved forms rather than from the diet. Furthermore, they showed  
392 that *P. annandalei* had a higher Ni excretion rate than *E. affinis* when copepods were exposed to  
393 dissolved forms and similar Ni excretion rates when copepods were exposed to the diet. According to  
394 these considerations, we might suggest that the low bNi concentrations in the northern coastal zone  
395 could be due to a better homeostasis regulation by planktonic species preferentially feeding on dissolved  
396 Ni. Further investigations are necessary to better understand how Ni impacts planktonic food webs in  
397 anthropized ecosystems.

398 Biotic V concentrations showed a two-modal distribution profiles in the three geographical areas  
399 with maxima values for F4 (~ 12  $\mu\text{g/g}$ ) in the northern coastal zone, for F2 and F6 (~ 2.5  $\mu\text{g/g}$ ) in the  
400 offshore zone, and for F2 (~ 7.5  $\mu\text{g/g}$ ) in the southern coastal zone. No significant differences in bV  
401 concentrations were found between the three geographical areas. V is an anthropogenic element that  
402 comes mainly from fossil fuel combustion, increasing globally by ~ 9% per year (Schlesinger et al.,  
403 2017). V enters the oceans through atmospheric deposition and is rapidly solubilised (Desboeufs et al.,  
404 2005). In oceans, V presents vertical profiles implying vertical transport by biological cycling (Jeandel



405 [et al., 1987](#), [Sherrel and Boyle, 1988](#)). Therefore, our results suggest that bV concentrations could be  
406 due to the atmospheric regional deposition of V in the Mediterranean Sea.

407 Biotic Zn concentrations followed the typical variations already observed for bCd, bCu, bFe and  
408 bNi (a bell-shaped distribution in the northern coastal zone, a flat-shaped in the offshore zone and an  
409 increasing gradient in the southern coastal zone) with the highest values for F5 at ~ 125 µg/g in the  
410 northern coastal zone, ~ 150 µg/g in the offshore zone, and ~ 110 µg/g in the southern coastal zone. No  
411 significant differences in bZn concentrations were found between the northern and southern coastal  
412 zones, but significant differences in bZn concentrations were found between the northern coastal zone  
413 and offshore zone and between the offshore zone and the southern coastal zone. Zn is an essential  
414 element, particularly for eukaryotes, but can readily be replaced by Cd or Co depending on the resident  
415 phytoplanktonic communities ([Morel, 2008](#)). The primary role of Zn (and Co, Cd) is to uptake inorganic  
416 carbon and fix it in the cells ([Hudson et al., 1993](#)). Since phytoplankton can adapt their Zn requirements  
417 to environmental conditions, even at low concentrations, the limitation of primary production by Zn is  
418 anecdotal ([Fritzwater et al., 2000](#); [Whitfield, 2001](#)). No specific behaviour of Zn could be observed in  
419 the three geographical areas. Our results suggest the absence of Zn limitation in Mediterranean Sea.

420

### 421 *3.22 Non-essential elements*

422 Non-essential elements showed very different distribution patterns within the geographical areas  
423 ([Fig. 3](#)). Biotic As presented a bell-shaped distribution in the northern coastal zone and an increasing  
424 gradient in the southern coastal zone with a maximum in F5 (~ 10 µg/g). In the offshore zone, bAs  
425 concentrations showed the highest variability with two high values in F2 and F5 fractions (~ 20 µg/g).  
426 No significant differences were found between the northern coastal zone and the offshore zone, but  
427 significant differences were found between the northern and southern coastal zones and between the  
428 offshore zone and the southern coastal zone. Arsenic is a metalloid biochemically similar to P and  
429 accumulates in planktonic food webs during adenotriphosphate cycle ([Wurl et al., 2013](#)). The  
430 distribution and concentration of chemical forms of As vary according to the trophic position or the  
431 ability of marine organisms to biotransform As ([Wrench et al., 1979](#); [Fattorini et al., 2006](#)). In marine  
432 ecosystems, As inputs are mainly from rivers affected by mine drainage and the phosphate fertiliser

433 industry (Elbaz-Poulichet, 2005). Since 1972, several phosphate fertiliser plants have been set up in  
434 coastal industrial cities (Sfax, Skhira and Gabès) of the Gulf of Gabès (El Zrelli et al., 2018; Feki-  
435 Sahnoun et al., 2019; Gargouri et al., 2021). Moreover, As is also present in a many compound such as  
436 pesticides, fertilizers, piles, paints, *etc.* (Warnau et al., 2006). According to these considerations, in the  
437 northern and southern coastal zones, we can speculate that lower bAs concentrations could be due to a  
438 better homeostasis regulation of As by planktonic food webs. Conversely, offshore, the Mediterranean  
439 Sea are nutrient-limited, which is less common in the western basin but is generally due to a lack of  
440 phosphate rather than nitrate (Krom et al., 2010; Pujo-Pay et al., 2011; Lazzari et al., 2016). In response  
441 to phosphate limitation, Arsenic can be converted to organic forms and excreted *via* methionine  
442 metabolism (Maher and Butler, 1988; Uthus, 2003; Du et al., 2021). In this context, we can speculate  
443 that high bAs concentrations in the offshore zone could be due to P-substitution, the two-modal  
444 distribution showing competition between metabolic processes of nanoeukaryotes (F2) and copepods  
445 (F5).

446 Biotic Cr presented contrasted distribution in the three geographical areas. In the northern  
447 coastal zone, bCr concentrations showed two high values in F3 (~ 7.5 µg/g) and in F6 (~ 15 µg/g). In  
448 the offshore zone, bCr concentrations decreased with increasing size fractions (from ~ 5 to 0.3 µg/g).  
449 Conversely, in the southern coastal zone, bCr concentrations increased with increasing size fractions  
450 (from ~ 2.5 to 10 µg/g). No significant differences were found between the northern and southern coastal  
451 zones, but significant differences were found between the northern coastal zone and offshore zone and  
452 between the offshore zone and the southern coastal zone. In marine environments, Cr mainly exists in  
453 trivalent (Cr<sup>III</sup>) and hexavalent (Cr<sup>VI</sup>) forms. Cr<sup>III</sup> can be adsorbed on plankton but hardly transferred to  
454 planktonic food webs (Pettine, 2000). In contrast, Cr<sup>VI</sup> is highly soluble and readily incorporated into  
455 planktonic cells through strong oxidative pathways by reacting with nucleic acids and proteins (Levina  
456 and Lay, 2008). In the offshore zone, the decrease of bCr might be partly explained by Cr excretion *via*  
457 dietary pathway and a possible 'bio-dilution' effect due to the decrease surface/volume ratio in higher  
458 trophic level organisms. According to previous studies (Dumas et al., 2015; Chifflet et al., 2019), the  
459 increase of bCr in the northern and southern coastal zones could be linked to local Cr anthropogenic

460 inputs. Differences between bCr distribution profiles in offshore and coastal zones would require  
461 additional study due to their impact on organisms.

462 Biotic Sb presented a bell-shaped distribution with high values in F5 (~ 10 µg/g) for the offshore  
463 zone and in F4 (~ 8 µg/g) for the southern coastal zone. Conversely, bSb concentrations were < 1 µg/g  
464 in the northern coastal zone. No significant differences were found between the offshore zone and  
465 southern coastal zones, but significant differences were found between the northern coastal zone and  
466 offshore zone and between the northern and southern coastal zones. Sb showed conservative profiles in  
467 the northernmost western Mediterranean Sea and, enriched surface profiles around the Strait of Sicily  
468 probably related to atmospheric deposition (Takayanagi et al., 1996). Sb is present in oxic seawaters as  
469 inorganic Sb<sup>III+V</sup> and methylated species especially in surface waters (Andrea and Froelich, 1984; Cutter  
470 and Cutter, 2006). According to the same authors, its biogeochemical cycle is controlled by biogenic  
471 uptake, particle scavenging, and regeneration processes. Thus, we can be assumed that geographical  
472 differences in bSb arise from differences in Sb atmospheric deposition and/or Sb speciation.

473

### 474 *3.3 Biomagnification of metals and metalloids*

475 Various concepts have been mobilised to assess the transfer of metals and metalloids in trophic  
476 food webs. Bioconcentration is the absorption of an element into an organism directly from the water  
477 through cell membranes. Bioaccumulation refers to the increase of an element in an organism over its  
478 lifetime from both the environment and food consumption. To complete these metrics, biomagnification  
479 is the increase in the concentration of an element in organisms from prey to predators. While  
480 bioconcentration and bioaccumulation describe the increase in concentration of an element in an  
481 organism exposed to its environment, biomagnification can be viewed as the increase in the  
482 concentration of an element throughout food webs (US EPA 2007; OECD, 2012).

483 To focus on the objectives of the MERITE-HIPPOCAMPE campaign (contaminant transfer in  
484 planktonic food webs), we used the TMF (trophic magnification factor) model to explore the  
485 biomagnification of metals and metalloids in the Mediterranean Sea. TMF values were presented per  
486 geographical area and element, and statistical measures ( $r^2$ ) indicated how the TMF model fit with values  
487 (Table 3).

488

489 *3.31 Essential elements*

490 TMF values for Cd were 3.9, 1.1 and 7.5 for the northern coastal, offshore and southern coastal  
491 zones, respectively. Due to multiple factors such as diet, excretion and biodilution, Cd does not  
492 biomagnify in high TL, but an opposite trend can be observed with lower TL under certain conditions  
493 (Liu et al., 2019; Annabi-Trabelsi et al., 2021). For example, *Cyanophyceae*, copepods, cephalopods,  
494 and crustaceans are the most Cd-sensitive species, and can accumulate Cd when nutrient inputs increase  
495 (Bai et al., 2022). The northern and southern coastal waters are influenced by both nutrients and Cd  
496 inputs from urban/industrial activities (Grousset et al., 1995; Teissier et al., 2011; Pasqueron de  
497 Fommervault et al., 2015; Heimbürger et al., 2013; El Zrelli et al., 2018; Feki-Sahnoun et al., 2019;  
498 Annabi-Trabelsi et al., 2022). According to these considerations, high TMF in the northern and southern  
499 coastal zones could possibly be sustained by local nutrients inputs.

500 TMF values for Cu were 2.2, 1.1 and 6.6 for the northern coastal, offshore and southern coastal  
501 zones, respectively. Cu is a micronutrient that plays a key role in primary production but it can also have  
502 a negative effect in planktonic species when dissolved Cu exceeds 10 pM (Brand et al., 1986; Peers et  
503 al., 2005). To prevent the negative effects, metallothionein and metallothionein-like proteins regulate  
504 the uptake, accumulation and excretion rates of certain elements in species (Nfon et al., 2009).  
505 Therefore, the low TMF (1.1) in the offshore zone could be explained by better homeostasis regulation  
506 of Cu in the species, thus indicating healthy planktonic webs. Conversely, high TMF values in northern  
507 and southern coastal zones can probably be due to high organic and mineral inputs to these waters due  
508 to the proximity to land.

509 TMF values for Fe were found at 1.4, 2.0 and 9.6 in the northern coastal, offshore and southern  
510 coastal zones, respectively. Due to its implication in nitrite reductase, Fe uptake is high when  
511 phytoplankton feed on nitrate rather than on ammonium (Milligan and Harrison, 2000). The high TMF  
512 in the southern coastal zone could possibly be influenced by the nitrogen forms originating from the  
513 Saharan dust (Khammeri et al., 2018) and local anthropogenic activities (El Zrelli et al., 2018; Chifflet  
514 et al., 2019; Feki-Sahnoun et al., 2019; Gargouri et al., 2021). Indeed, in the Gulf of Gabès, both  
515 diazotrophic cyanobacteria (*Anabaena sp.*, *Chlorococcus sp.*, *Trichodesmium erythraeum*, *Spirulina sp.*

516 and *Spirulina subsalsa*) and non-diazotrophic cyanobacteria (*Pseudoanabaena sp.* and *Microcystis sp.*)  
517 showed great flexibility in nitrogen assimilation, allowing algal blooms (Drira et al., 2017). The Gulf of  
518 Gabès is considered a highly productive area (D'Ortenzio and d'Alcalà, 2009; Ben Brahim et al., 2010).  
519 Conversely, the northern coastal zone does not have a high TMF value (1.4) despite atmospheric inputs  
520 (Guieu et al., 1997) and the influence of Rhône river inputs (Ollivier et al., 2011). As suggested in the  
521 previous section, Fe could appear as a co-factor of planktonic activity and its transfer in planktonic food  
522 webs might be species-dependent.

523 Mn presented few differences in TMF values with respect to geographical areas: 2.7 in the  
524 northern coastal zone, 2.0 in the offshore and, 1.2 in the southern coastal zones. Like Fe, Mn is an  
525 essential element involved in oxygen transport during photosynthesis (Bruland and Lohan, 2003). Mn  
526 biomagnification is poorly documented but is likely depend on both size and species composition  
527 (Battuello et al., 2016). In coastal ecosystems where concentrations of dissolved metals can be higher  
528 than in the offshore zone, there is a homeostasis regulation in cells with decreasing affinity for Mn and  
529 increasing affinity for Cu and Zn *via* metalloproteins (especially the metallothionein group) activity,  
530 thereby limiting Mn biomagnification (Whitfield, 2001). The few differences in Mn biomagnification  
531 could possibly be explained by the rate of Mn intake and the rate of Mn utilisation in the biochemical  
532 processes

533 TMF values for Ni were found at 1.6, 0.9 and 3.8 for the northern coastal, offshore and southern  
534 coastal zones, respectively. Same trends were also observed for Zn (2.5, 1.2 and 4.7 for the northern  
535 coastal, offshore and southern coastal zones, respectively). Metals transfers in planktonic food webs  
536 result from passive (adsorption and diffusion) and active uptake mechanisms controlled by the  
537 bioavailability of elements (Morel et al., 2003; Sunda, 2012). As previously observed, copepods (mainly  
538 in F5) play a key role in bM distribution. Indeed, the feeding of copepods can be based both on the  
539 absorption of dissolved substances and on the consumption of prey (Wang et al., 2002; Battuello et al.,  
540 2017). Coastal ecosystems are particularly sensitive to environmental variations (temperature, pH,  
541 salinity, nutrients, dissolved organic matter, light) that also influence the bioavailability of metals and  
542 metalloids (Sunda, 2012). Therefore, the biomagnification of Ni and Zn could depend on different  
543 environmental conditions between the three geographical areas, and the high TMF values in the southern

544 coastal zone could indicate active biological uptake in this area. The findings agree with [Madgett et al.](#)  
545 [\(2021\)](#) who suggested a species-specific accumulation of Ni and Zn rather than biomagnification in  
546 trophic food webs (zooplankton, invertebrate, fish).

547 TMF values for V in the offshore and southern coastal zones (0.9 and 1.3, respectively) showed  
548 no biomagnification. However, in the northern coastal zone, we observed abnormally high bV  
549 concentrations at St4 (Table S3) possibly showing local contamination associated with fossil fuel  
550 combustion ([Pacyna and Pacyna, 2001](#); [Schlesinger et al., 2017](#)). We therefore assessed the TMF of V  
551 using only data from St1–3 (2.2), which was more representative of this geographical area.  
552 Biomagnification of V is poorly documented in copepods but biomagnification of V was already  
553 observed in crustaceans ([Asante et al., 2008](#)). In the present study, decreasing bV concentrations were  
554 recorded in F6 and F7 fractions of the three geographical areas. This general pattern could be explained  
555 by a possible biodilution effect with increasing species size. However, high bV concentrations were  
556 found in the nearshore station of Marseilles bay (St4), where the impact of fossil fuel combustion on  
557 trophic food webs should be further investigated.

558

### 559 *3.32 Non-essential elements*

560 TMF values for As were 1.1, 1.3 and 3.9 for the northern coastal, offshore and southern coastal  
561 zones, respectively. In marine environment, trophic food webs show biodilution of As becoming  
562 significant at low phosphate concentrations ([Cutter et al., 2001](#)). Mean phosphate concentrations  
563 measured at the DCM depth in the MERITE-HIPPOCAMPE campaign were found at 0.09, 0.05 and  
564 0.22  $\mu\text{M}$  in the northern coastal, offshore and southern coastal zones, respectively ([Tedetti et al., 2022](#)).  
565 Under low phosphate concentrations, As can be converted to organic forms and excreted ([Maher and](#)  
566 [Butler, 1988](#); [Uthus, 2003](#); [Du et al., 2021](#)). This metabolism would limit As biomagnification in the  
567 offshore and northern coastal zones. Conversely, in the southern coastal zone, the Gulf of Gabès is  
568 surrounded by phosphate-industry plants that enrich the coastal waters through dust deposits or  
569 wastewater discharge ([El Zrelli et al., 2018](#); [Chifflet et al., 2019](#); [Feki-Sahnoun et al., 2019](#); [Gargouri et](#)  
570 [al., 2021](#)), which could favour As biomagnification in this area.

571 Higher TMF values were observed for Cr in the northern (2.1) and southern (5.8) coastal zones  
572 compared to the offshore zone (0.8). While negative effects of Cr on cellular metabolism are well known  
573 (Levina and Lay, 2008), its transfer into the TL is poorly documented. Despite high bCr concentrations  
574 (~ 15 µg/g) at F6 (large copepods and small crustaceans), a moderate TMF (2.1) was found in the  
575 northern coastal zone. Previous studies have suggested that phytoplankton can assimilate Cr by  
576 extracellular adsorption and sequester it in their cells (Rentería-Cano et al., 2011; Semeniuk et al., 2016).  
577 Our study shows that despite Cr inputs from the anthropogenic activities of the cities of Marseilles and  
578 Toulon (Tessier et al., 2011; Dumas et al., 2015), excretion and biodilution might partly explain the  
579 lower concentrations in zooplankton, thus limiting Cr biomagnification in the northern coastal zone.  
580 However, in the southern coastal zone, we found a high TMF (5.8) with a moderate bCr (~ 5 µg/g). This  
581 geographical area is highly impacted by anthropogenic activities with recurrent metals and metalloids  
582 contamination (El Zrelli et al., 2018; Chifflet et al., 2019; Feki-Sahnoun et al., 2019; Gargouri et al.,  
583 2021). In Gdańsk Bay (Poland), Cr bioaccumulation is taxon-specific, with high concentrations for  
584 copepods (Pempkowiak et al., 2006). According to our results, under stressful conditions, Cr  
585 biomagnification may no longer be controlled by homeostasis regulation and be species-dependent,  
586 leading to increased Cr concentrations in planktonic food webs.

587 TMF values for Sb were found at 3.1, 1.3 and 5.7 for the northern coastal, offshore and southern  
588 coastal zones, respectively. Sb biomagnification in the planktonic food web is poorly documented, and  
589 to our knowledge the only existing work is in freshwater ecosystems. Sb biomagnification is species-  
590 dependent and governed by trophic ecology (Filella et al., 2002). Sb does not biomagnify in primary  
591 predators or with the upper TL, but there may be biomagnification processes in autotrophic and  
592 heterotrophic organisms under anthropogenic pressure (Obiakor et al., 2017). Our results show high  
593 TMF in the northern and southern coastal zones. Further investigation would greatly improve our  
594 understanding of the transfer and bioaccumulation processes of Sb on the marine planktonic community  
595 in anthropogenic ecosystems.

596

597

598 **3. Conclusions**

599 This study evaluated the transfer of metals and metalloids in planktonic food webs (from  
600 bacteria to zooplankton) along a North-South Mediterranean transect. Discrimination between biotic  
601 (living and dead organic matter and faecal pellets) and geogenic (authigenic and lithogenic matter)  
602 components was used to determine concentrations of metals and metalloids bound to the planktonic  
603 network. Biotic metals and metalloids concentrations (except Cr, Mn, and V) were higher in the offshore  
604 zone than in the coastal zones. In addition, biotic Sb and V concentrations appeared to be affected by  
605 atmospheric deposition, and biotic Cr concentrations appeared to be affected by local anthropogenic  
606 inputs. While essential elements (Cd, Cu, Fe, Mn, Ni, V, Zn) showed similar patterns of distribution  
607 controlled by nanoeukaryotes and copepods, non-essential elements (As, Cr, Sb) showed variable  
608 distributions depending on their biochemical characteristics, environmental conditions and the structure  
609 of plankton communities. Metals and metalloids were not biomagnified in the offshore zone, probably  
610 due to homeostasis regulatory processes in organisms. On the contrary, planktonic food webs presented  
611 high biomagnification factors in the northern and southern coastal waters possibly caused by  
612 anthropogenic inputs. An excess of non-essential elements can inhibit cell development and nutrient (C,  
613 N, P) inputs can improve productivity. Due to these synergistic and antagonistic interactions, more  
614 complete consideration should be given in the future to understand the interactive effects between metals  
615 and metalloids inputs and plankton growth. For example, in the southern coastal zone, anthropogenic  
616 inputs of As, Cd, Cu, Cr and Sb and nutrients could modify the interactions between species and promote  
617 metals and metalloids transfers into planktonic food webs. The impact of geogenic inputs on Cu and Zn  
618 biogeochemical cycles was studied in more detail using Cu and Zn isotopic compositions in a companion  
619 paper ([Chifflet et al., 2022](#)) in order to improve our understanding of the transfer of metals and  
620 metalloids in the planktonic network.

621

622

623 **Supplementary information.** The supplementary material related to this article is available online at  
624 XXX.

625



626 **Author contribution.** All the authors participated in the MERITE-HIPPOCAMPE project and  
627 contributed to the sampling strategy, preparation of the material, field work, laboratory analyses and/or  
628 data processing and interpretation. SC and NB wrote the original manuscript, and all the authors  
629 participated to its reviewing and/or editing.

630

631 **Acknowledgments.** The MERITE-HIPPOCAMPE project was initiated and funded by the cross-  
632 disciplinary “Pollution & Contaminants” axis of the CNRS-INSU MISTRALS program (joint action of  
633 the MERMEX-MERITE and CHARMEEX subprograms). The project also received the financial support  
634 from the Franco-Tunisian International Joint Laboratory (LMI) COSYS-Med. The MERITE-  
635 HIPPOCAMPE campaign was organized and supported by the French Oceanographic Fleet,  
636 CNRS/INSU, IFREMER, and IRD, the Tunisian Ministry of Agriculture, Water Resources and  
637 Fisheries, and the Tunisian Ministry of Higher Education and Scientific Research. The project also  
638 received additional funding from the MIO’s “Action Sud” and “Transverse” incentive programs  
639 (CONTAM project) and by the ANR-sponsored CONTAMPUMP project (ANR JCJC #19-CE34-0001-  
640 01). We thank E. de Saint-Léger (DT-INSU, Brest) for provisioning the *in-situ* McLane pumps with  
641 sequential filtration units. We also thank the MIO platform “Service Atmosphère-Mer” (SAM) for  
642 preparation and management of the embarked material and the MIO “Plateforme Analytique de Chimie  
643 des Environnements Marins” (PACEM platform) and the staff at the LBCM-Ifremer laboratory for  
644 performing various chemical analyses. The authors are deeply grateful for the thorough and constructive  
645 corrections and insightful comments of the guest editor and the anonymous reviewers, who have  
646 significantly improved the original manuscript.

647

648 **References**

- 649 Aminot, A., K erouel, R., Coverly, S., 2009. Nutrients in seawater using segmented flow analysis. In O.  
650 Wurl, O., (Ed.), Practical guidelines for the analysis of seawater, 408p, CRC Press
- 651 Andreae, M.O., Froelich, P.N., 1984. Arsenic, antimony and germanium biochemistry in the Baltic Sea.  
652 Tellus, 36B, 101-117.
- 653 Annabi-Trabelsi, N., Guermazi, W., Karam, Q., Ali, M., Uddin, S., Leignel, V., Ayadi, H., 2021.  
654 Concentrations of trace metals in phytoplankton and zooplankton in the Gulf of Gab es, Tunisia. Mar.  
655 Pollut. Bull., 168, 112392.
- 656 Annabi-Trabelsi, N., Guermazi, W., Leignel, V., Al-Enezi, Y., Karam, Q., Ali, M., Ayadi, H., Belmonte,  
657 G., 2022. Effects of Eutrophication on Plankton Abundance and Composition in the Gulf of Gab es  
658 (Mediterranean Sea, Tunisia). Waters, 14, 2230.
- 659 Asante, K.A., Agusa, T., Mochizuki, H., Ramu, K., Inoue, S., Kubodera, T., Takahashi, S.,  
660 Subramanian, A., Tanabe, S., 2008. Trace elements and stable isotope ( $\delta^{13}\text{C}$  and  $\delta^{15}\text{N}$ ) in shallow  
661 and deep-water organisms from the East China Sea. Environ. Pollut., 156, 862-873.
- 662 Ayata, S.D., Irisson, J.O., Aubert, A., Berline, L., Dutay, J.C., Mayot, N., Nieblas, A.E., D'Ortenzio, F.,  
663 Palmieri, J., Reygondeau, G., Rossi, V., Guieu, C., 2018. Regionalisation of the Mediterranean basin,  
664 a MERMEX synthesis. Progr. Oceanogr., 163, 7-20.
- 665 Bai, X., Jiang, Y., Jiang, Z., Zhu, L., Feng, J., 2022. Nutrient potentiate the responses of plankton  
666 community structure and metabolites to cadmium: A microcosm study. J. Hazard. Mater., 430,  
667 128506.
- 668 Barka, S., Pavillon, J.F., Amiard-Triquet, C., 2010. Metal distributions in *Tigriopus brevicornis*  
669 (Crustacea, Copepoda) exposed to copper, zinc, nickel, cadmium, silver, and mercury, and  
670 implication for subsequent transfer in the food web. Environ. Toxicol., 25, 350-360
- 671 Battuello, M., Brizio, P., Mussat, Sartor, R., Nurra, N., Pessani, D., Abete, M.C., Squadrone, S., 2016.  
672 Zooplankton from a North Western Mediterranean area as a model of metal transfer in a marine  
673 environment. Ecol. Indic., 66, 440-451.

674 Battuello, M., Sartor, R.M., Brizio, P., Nurra, N., Pessani, D., Abete, M.C., Squadrone, S., 2017. The  
675 influence of feeding strategies on trace element bioaccumulation in copepods (*Calanoida*). Ecol.  
676 Indic., 74, 311-320.

677 Béjaoui, B., Ben Ismail, S., Othmani, A., Ben Abdallah-Ben Hadj Hamida, O., Chevalier, C., Feki-  
678 Sahnoun, W., Harzallah, A., Ben Hadj Hamida, N., Bouaziz, R., Dahech, S., Diaz, F., Tounsi, K.,  
679 Sammari, C., Pagano, M., Bel Hassen, M., 2019. Synthesis review of the Gulf of Gabes (eastern  
680 Mediterranean Sea, Tunisia): morphological, climatic, physical oceanographic, biogeochemical and  
681 fisheries features. Estuar. Coast. Shelf Sci., 219, 395-408.

682 Ben Brahim, M., Hamza, A., Hannachi, I., Rebai, A., Jarboui, O., Bouain, A., Aleya, L., 2010.  
683 Variability in the structure of epiphytic assemblages of *Posidonia oceanica* in relation to human  
684 interferences in the Gulf of Gabes, Tunisia. Mar. Environ. Res. 70, 411-421.

685 Bianchi, C.N., Morri, C., 2000. Marine biodiversity of the Mediterranean Sea: situation, problems and  
686 prospects for future research. Mar. Pollut. Bull., 40, 367-376.

687 Bishop, J.K.B., Lam, P.J., Wood, T.J., 2012. Getting good particles: Accurate sampling of particles by  
688 large volume in-situ filtration. Limnol. Oceanogr., 10, 681-710.

689 Borgå, K., Kidd, K.A., Muir, D.C.G., Berglund, O., Conder, J.M., Gobas, F.A.P.C., Kucklick, J., Malm,  
690 O., Powell, D.E., 2012. Trophic magnification factors: Considerations of ecology, ecosystems and  
691 study design. Integr. Environ. Assess. Manag., 8, 64-84.

692 Boudriga, I., Thyssen, M., Zouari, M., Garcia, N., Tedetti, M., Bel Hassen, M., 2022.  
693 Ultraphytoplankton community structure in subsurface waters along a North-South Mediterranean  
694 transect. Mar. Pollut. Bull., 182, 113977.

695 Brand, L.E., Sunda, W.G., Guillard, R.R.L., 1986. Reduction in marine phytoplankton reproduction  
696 rates by copper and cadmium. J. Exp. Mar. Biol. Ecol., 96, 225-250.

697 Bruland, K.W., Lohan, M.C., 2003. Control of trace metals in seawater. Treatise Geom., 6, 23-47.

698 Burkhard, L., Arnot, J.A., Embry, M.R., Farley, K.J., Hoke, R.A., Kitano, M., Leslie, H.A., Lotufo,  
699 G.R., Parkerton, T.F., Sappington, K.G., Tomy, G.T., Woodburn, K.B. 2011. Comparing laboratory  
700 and field measured bioaccumulation end points. IEAM, 8, 17-31.

701 Burton, J.D., Statham, P.J., 1990. Trace metals in seawater. In: Heavy Metals in the Marine Environment  
702 (Eds. P.S. Rainbow and R. W. Furness). CRC Press, Boca Raton, FL.

703 Campbell, L.M., Norstrom, R.J., Hobson, K.A., Muir, D.C.G., Backus, S., Fisk, A.T., 2005. Mercury  
704 and other trace elements in a pelagic Arctic marine food web (Northwater Polynya, Baffin Bay). *Sci.*  
705 *Tot. Environ.*, 351-352, 247-263.

706 Chester, R., Nimmo, M., Keyse, S., 1996. The influence of Saharan and Middle Eastern desert-derived  
707 dust on the trace metal composition of Mediterranean aerosols and rainwater: An Overview. In:  
708 Guerzoni, S., Chester, R. (eds). *Environmental Science and Technology Library*, 11. 253-273,  
709 Springer, New York.

710 Chevrollier, L.A., Koski, M., Søndergaard, J., Trapp, S., Aheto, D.W., Darpaah, G., Nielsen, T.G., 2022.  
711 Bioaccumulation of metals in the planktonic food web in the Gulf of Guinea. *Mar. Pollut. Bull.*, 179,  
712 113662.

713 Chifflet, S., Tedetti, M., Zouch, H., Fourati, R., Zaghden, H., Elleuch, B., Quéméneur, M., Karray, F.,  
714 Sayadi, S., 2019. Dynamics of trace metals in a shallow coastal ecosystem: insights from the Gulf of  
715 Gabès (southern Mediterranean Sea). *AIMS Environ. Sci.*, 6, 277-297.

716 Chifflet, S., Briant, N., Freydier, R., Araújo, D.F., Quéméneur, M., Zouch, H., Bellaaj-Zouari, A.,  
717 Carlotti, F., Tedetti, M. 2022. Isotopic compositions of Copper and Zinc in plankton from the  
718 Mediterranean Sea (MERITE-HIPPOCAMPE campaign): tracing trophic transfer and geogenic  
719 inputs. *Mar. Pollut. Bul.*, in revision, this special issue.

720 Chauvelon, T., Strady, E., Harmelin-Vivien, M., Radakovitch, O., Brach-Papa, C., Crochet, S., Knoery,  
721 J., Rozuel, E., Thomas, B., Tronczynski, J., Chiffolleau, J.F., 2019. Patterns of trace metal  
722 bioaccumulation and trophic transfer in a phytoplankton-zooplankton-small pelagic fish marine food  
723 web. *Mar. Pollut. Bull.*, 146, 1013-1030.

724 Collier, R., Edmond, J., 1984. The trace element geochemistry in marine biogenic particulate matter.  
725 *Progr. Oceanogr.*, 13, 113-199.

726 Cossa, D., Coquery, M., 2005. The Mediterranean mercury anomaly, a geochemical or a biological  
727 issue. In: Saliot, A. (Ed.), *The Mediterranean Sea. Handbook of Environmental Chemistry*, pp. 177-  
728 208.

729 Cossa, D., Knoery, J., Banaru, D., Harmelin-Vivien, M., Sonke, J.E., Hedgecock, I.M., Bravo, A.G.,  
730 Rosati, G., Canu, D., Horvat, M., Sprovieri, F., Pirrone, N., Heimbürger-Boavida, L.E., 2022.  
731 Mediterranean Mercury Assessment 2022: An Updated Budget, Health Consequences, and Research  
732 Perspectives. *Environ. Sci. Technol.*, 56, 3840-3862.

733 Croot, P.L., Moffett, J.W., Brand, L.E., 2000. Production of extracellular Cu complexing ligands by  
734 eukaryotic phytoplankton in response to Cu stress. *Limnol. Oceanogr.*, 45, 619-627.

735 Cullen, J., Sherrell, R.M., 1999. Techniques for determination of trace metals in small samples of size-  
736 fractionated particulate matter: Phytoplankton metals off central California. *Mar. Chem.*, 67, 233-  
737 247.

738 Cutter, G.A., Cutter, L.S., Featherstone, A.M., Lohrenz, S.E., 2001. Antimony and arsenic  
739 biogeochemistry in the western Atlantic Ocean. *Deep-Sea Res. II*, 48, 2895–2915.

740 Cutter, G.A., Cutter, L.S., 2006. Biogeochemistry of arsenic and antimony in the North Pacific Ocean.  
741 *Geochem, Geophys*, 7, 1-12.

742 Cutter, G., Casciotti, K., Croot, P., Geibert, W., Heimbürger, L.E., Lohan, M., Planquette H., Van de  
743 Flierdt, T., 2017. Sampling and sample-handling protocols for GEOTRACES cruises. *GEOTRACES*  
744 *Community Practices, Version 3*, 139 pp. & Appendices.

745 D’Ortenzio, F., d’Alcalà, M.R., 2009. On the trophic regimes of the Mediterranean Sea: a satellite  
746 analysis. *Biogeosciences*, 6, 139-148.

747 Damshäuser, A., Wagener, T., Garbe-Schönberg, D., Croot, P., 2013. Particulate and dissolved  
748 aluminum and titanium in the upper water column of the Atlantic Ocean. *Deep-Sea Res. I*, 73, 127-  
749 139.

750 Desboeufs, K.V., Sofikitis, A., Losno, R., Colin, J.L., Ausset, P., 2005. Dissolution and solubility of  
751 trace metals from natural and anthropogenic aerosol particulate matter. *Chemosphere*, 58, 195-203.

752 Donat, J. R., Bruland, K.W., 1995. Trace elements in the oceans. In: *Trace Elements in Natural Waters*  
753 (Eds. E. Steinnes and B. Salbu). CRC Press, Boca Raton, FL.

754 Drira, Z., Chaari, D., Hamza, A., Bel Hassen, M., Pagano, M., 2017. Diazotrophic cyanobacteria  
755 signatures and their relationship to hydrographic conditions in the Gulf of Gabes, Tunisia. *J. Mar.*  
756 *Biolog. Assoc. U.K.*, 97, 69-80.

757 Du, S., Zhou, Y., Zhang, L., 2021. The potential of arsenic biomagnification in marine ecosystems: A  
758 systematic investigation in Daya Bay in China. *Sci. Tot. Environ.*, 773, 145068.

759 Dumas, C., Ludwig, W., Aubert, D., Eyrolle, F., Raimbault, P., Gueneugues, A., Sotin, C., 2015.  
760 Riverine transfer of anthropogenic and natural trace metals to the Gulf of Lions (NW Mediterranean  
761 Sea). *Appl. Geochemistry*, 58, 14-25.

762 Dupont, C.L., Barbeau, K., Palenik, B., 2008. Ni uptake and limitation in marine *Synechococcus* strains.  
763 *Appl. Environ. Microbiol.*, 74, 23-31.

764 El Zreli, R., Rabaoui, L., Alaya, M.B., Daghbouj, N., Castet, S., Besso, P., Michel, S., Bejaoui, N.,  
765 Courjault-Radé, P., 2018. Seawater quality assessment and identification of pollution sources along  
766 the central coastal area of Gabes Gulf (SE Tunisia): Evidence of industrial impact and implications  
767 for marine environment protection. *Mar. Pollut. Bull.*, 127, 445-452.

768 Elbaz-Poulichet, F., 2005. River Inputs of Metals and Arsenic. In: Saliot, A. (Ed). *The Mediterranean*  
769 *Sea, Handbook of Environ. Chem.*, Springer, Berlin, 5, 211-235.

770 Fattorini, D., Notti, A., Regoli, F., 2006. Characterization of arsenic content in marine organisms from  
771 temperate, tropical, and polar environments. 22, 405-414.

772 Feki-Sahnoun, W., Njah, H., Barraji, N., Mahfoudi, M., Akrouf, F., Rebai, A., Bel Hassen, M., Hamza,  
773 A. 2019. Influence of phosphorus-contaminated sediments in the abundance of potentially toxic  
774 phytoplankton along the Sfax Coasts (Gulf of Gabes, Tunisia). *Journal of Sedimentary*  
775 *Environments*, 4, 458-470.

776 Fierro-González, P., Pagano, M., Guilloux, L., Makhoul, N., Carlotti F. 2022. Comparative  
777 zooplankton structure and functioning in epipelagic layers of different Mediterranean regions during  
778 the HIPPOCAMPE cruise. *Mar. Pollut. Bul.*, in preparation, this special issue.

779 Filella, M., Belzile, N., Chen, Y.W., 2002. Antimony in the environment: A review focused on natural  
780 waters. I. Occurrence. *Earth-Sci. Rev.*, 57, 125-176.

781 Fritzwater, S.E., Johnson, K.S., Gordon, R.M., Coale, K.H., Smith, W.O., 2000. Trace metal  
782 concentration in the Ross Sea and their relationship with nutrients and phytoplankton growth. *Deep*  
783 *Sea Res.*, 47, 3159-3179.

784 Gao, Y., Wang, R., Li, Y., Ding, X., Jiang, Y., Feng, J., Zhu, L., 2021. Trophic transfer of heavy metals  
785 in the marine food web based on tissue residuals. *Sci. Tot. Environ.*, 772, 145064.

786 Gargouri, D., Annabi-Trabelsi, N., Karam, Q., Ali, M., Ayadi, H., 2021. Assessment of metallic  
787 pollution in the waters, suspended particulate matter, and surface sediments of the central coastal  
788 area of the Gulf of Gabès, Mediterranean Sea. *J. Mater. Environ. Sci.*, 12, 584-594.

789 Goldberg, E.D., 1954. Marine Geochemistry 1. Chemical Scavengers of the Sea. *J. Geol.*, 62, 249-265.

790 Grousset, F. E., Quétel, C. R., Thomas, B., Donard, O. F. X., Lambert, C. E., Guillard, F., Monaco, A.,  
791 1995. Anthropogenic vs. lithogenic origins of trace elements (As, Cd, Pb, Rb, Sb, Sc, Sn, Zn) in  
792 water column particles: northwestern Mediterranean Sea. *Mar. Chem.*, 48, 291-310.

793 Guieu, C., Chester, R., Nimmo, M., Martin, J. M., Guerzoni, S., Nicolas, E., Mateu, J., Keyse, S., 1997.  
794 Atmospheric input of dissolved and particulate metals to the northwestern Mediterranean. *Deep Sea*  
795 *Res., Part II*, 44, 655 – 674

796 Guieu, C., Loÿe-Pilot, M.D., Ridame, C., Thomas, C., 2002. Chemical characterization of the Saharan  
797 dust end-member: Some biogeochemical implications for the western Mediterranean Sea. *J.*  
798 *Geophys. Res.*, 107 (D15), 4258.

799 Guieu, C., Loÿe-Pilot, M.D., Benyaya, L., Dufour, A., 2010. Spatial variability of atmospheric fluxes of  
800 metals (Al, Fe, Cd, Zn and Pb) and phosphorus over the whole Mediterranean from a one-year  
801 monitoring experiment; biogeochemical implications. *Mar. Chem.*, 120, 164-178.

802 Hazen, E.L., Abrahms, B., Brodie, S., Carroll, G., Jacox, M.G., Savoca, M.S., Scales, K.L., Sydeman,  
803 W.J., Bograd, S.J., 2019. Marine top predators as climate and ecosystem sentinels. *Front. Ecol.*  
804 *Environ.* 17, 565-574

805 Heimbürger, L.E, Migon, C., Dufour, A., Chiffolleau, F., Cossa, D., 2010. Trace metal concentrations in  
806 the North-western Mediterranean atmospheric aerosol between 1986 and 2008: Seasonal patterns  
807 and decadal trends. *Sci. Tot. Environ.*, 408, 2629-2638.

808 Heimbürger, L.E., Mignon, C., Cossa, D., 2011. Impact of atmospheric deposition of anthropogenic and  
809 natural trace metals on Northern Mediterranean surface waters: A box model assessment. *Environ.*  
810 *Pollut.*, 159, 1629-1634.

811 Heimbürger, L.E, Lavigne, H., Migon, C., D'Ortenzio, F., Estournel, C., Coppola, L., Miquel, J.C.,  
812 2013. Temporal variability of vertical export flux at the DYFAMED time-series station  
813 (Northwestern Mediterranean Sea). *Progr. Oceanogr.*, 119, 59-67.

814 Ho, T.Y., Quigg, A., Finkel, Z.V., Milligan, A.J., Wyman, K., Falkowski, P.G., Morel, F.M.M, 2003.  
815 The elemental composition of some marine phytoplankton. *J. Phycol.*, 39, 1145-1159.

816 Ho, T.Y., Wen, L.S., You, C.F., Lee, D.C., 2007. The trace metal composition of size-fractionated  
817 plankton in the South China Sea: Biotic versus abiotic sources. *Limnol. Oceanogr.*, 52, 1776-1788.

818 Ho, T.Y., Chou, W.C., Wei, C.L., Lin, F.J, Wong, G.T.F., Lin, H.L., 2010. Trace metal cycling in the  
819 surface water of the South China Sea: Vertical fluxes, composition, and sources. *Limnol. Oceanogr.*,  
820 55, 1807-1820.

821 Hudson, R.J.M., Morel, F.M.M., 1993. Trace metal transport by marine microorganisms. Implications  
822 of metal coordination kinetics. *Deep Sea Res. Part I*, 40, 129-150.

823 Hunt, B.P.V., Carlotti, F., Donoso, K., Pagano, M., D'Ortenzio, F., Taillandier, V., Conan, P., 2017.  
824 Trophic pathways of phytoplankton size classes through the zooplankton food web over the spring  
825 transition period in the north-west Mediterranean Sea. *J. Geophys. Res.*, 122, 6309–6324.

826 Jeandel, C., Caisso, M., Minster, J.F., 1987. Vanadium behavior in the global ocean and in the  
827 Mediterranean Sea. *Mar. Chem.*, 21, 51-74.

828 Jordi, A., Basterretxea, G., Tovar-Sánchez, A., Alastuey, A., Querol, X., 2012. Copper aerosols inhibit  
829 phytoplankton growth in the Mediterranean Sea. *PNAS*, 109, 21246-21249.

830 Kadiene, E.U., Ouddane, B., Hwang, J.S., Souissi, S., 2019. Bioaccumulation of metals in calanoid  
831 copepods by oral intake. *Sci. Rep.*, 9, 9492.

832 Khammeri, Y., Hamza, I.S., Bellaaj-Zouari, A., Hamza, A., Sahli, E., Akrouf, F., Ben Kacem, M.Y.,  
833 Messaoudi, S., Bel Hassen, M., 2018. Atmospheric bulk deposition of dissolved nitrogen,  
834 phosphorus and silicate in the Gulf of Gabès (South Ionian Basin); implications for marine  
835 heterotrophic prokaryotes and ultraphytoplankton. *Cont. Shelf Res.*, 159, 1-11.

836 Kidd, K.A., Burkhard, L.P., Babut, M., Borgå, K., Muir, D., Perceval, O., Ruedel, H., Woodburn, K.,  
837 Embry, M.R., 2018. Practical advice for selecting or determining trophic magnification factors for



838 application under the European Union Water Framework Directive. *Integr. Environ. Assess. Manag.*,  
839 15, 266-277.

840 Krom, M. D., Emeis, K.-C., and Cappellen, P. V., 2010. Why is the Eastern Mediterranean phosphorus  
841 limited? *Prog. Oceanogr.*, 85, 236-244.

842 Lane, T.W., Morel, F.M.M., 2000. A biological function for cadmium in marine diatoms. *PNAS*, 97,  
843 46627-4631.

844 Lazzari, P., Solidoro, C., Salon, S., Bolzon, G., 2016. Spatial variability of phosphate and nitrate in the  
845 Mediterranean Sea: A modeling approach. *Deep-Sea Res.*, 108, 39-52.

846 Leblanc, K., Quéguiner, B., Diaz, F., Cornet, V., Michel-Rodriguez, M., Durrieu de Madron, X., Bowler,  
847 C., Malviya, S., Thyssen, M., Gregori, G., Rembauville, M., Grosso, O., Poulain, J., de Vargas, C.,  
848 Pujo-Pay, M., Conan, P., 2018. Nanoplanktonic diatoms are globally overlooked but play a role in  
849 spring blooms and carbon export. *Nature Communication*, 9, 953.

850 Lee, J.G., Roberts, S.B., Morel, F.M.M., 1995. Cadmium: A nutrient for the marine diatom  
851 *Thalassiosira weissflogli*. *Limnol. Oceanogr.*, 40, 1056-1063.

852 Lefevre, D., Mins, H.J., Robinson, C., Williams, P.J. Le B., Woodward, E.M.S., 1997. Review of gross  
853 community production, primary production, net community production and dark community  
854 respiration in the Gulf of Lions. *Deep Sea Res. II*, 44, 801-832.

855 Lemaitre, N., Planquette, H., Dehairs, F., Planchon, F., Sarthou, G., Gallinari, M., Roig, S., Jeandel, C.,  
856 Castrillejo, M., 2020. Particulate Trace Element Export in the North Atlantic (GEOTRACES GA01  
857 Transect, GEOVIDE Cruise). *ACS Earth Space Chem.*, 4, 2185-2204.

858 Levina, A., Lay, P., 2008. Chemical properties and toxicity of chromium (III) nutritional supplements.  
859 *Chem. Res. Toxicol.*, 21, 563-571.

860 Liao, W.H., Yang, S.C., Ho, T.Y., 2017. Trace metal composition of size-fractionated plankton in the  
861 Western Philippine Sea: The impact of anthropogenic aerosol deposition. *Limnol. Oceanogr.*, 62,  
862 2243-2259.

863 Liu, J., Cao, L., Dou, S., 2019. Trophic transfer, biomagnification and risk assessments of four common  
864 heavy metals in the food web of Laizhou Bay, the Bohai Sea. *Sci. Tot. Environ.*, 670, 508-522.

865 Madgett, A.S., Yates, K., Webster, L., McKenzie, C., Moffat, C.F., 2021. The concentration and  
866 biomagnification of trace metals and metalloids across four trophic levels in a marine food web. *Mar.*  
867 *Pollut. Bull.*, 173, 112929.

868 Maher, W., Butler, E., 1988. Arsenic in the marine environment. *Appl. Oceanogr. Chem.*, 2, 191-214.

869 Martin, J.M., Whitfield, M., 1983. The significance of the river input of chemical elements to the ocean.  
870 In: Wong, C.S., Boyle, E., Bruland, K.W., Burton, J.D., Goldberg, E.D., (Ed). *Trace Metals in*  
871 *Seawater*. Plenum, New York, 265-296.

872 Marañón, E., Wambeke, F., Uitz, J., Boss, E., Dimier, C., Dinasquet, J., Engel, A., Haëntjens, N., Pérez-  
873 Lorenzo, M., Taillandier, V., Zäncker, B., 2021. Deep maxima of phytoplankton biomass, primary  
874 production and bacterial production in the Mediterranean Sea. *Biogeosciences*, 18, 1749-1767.

875 Maxwell, S.M., Hazen, E.L., Bograd, S.J., Halpern, B.S., Breed, G.A., Nickel, B., Teutschel, N.M.,  
876 Crowder, L.B., Benson, S., Dutton, P.H., Bailey, H., Kappes, M.A., Kuhn, C.E., Weise, M.J., Mate,  
877 B., Shaffer, S.A., Hassrick, J.L., Henry, R.W., Irvine, L., McDonald, B.I., Robinson, P.W., Block,  
878 B.A., Costa, D.P., 2013. Cumulative human impacts on marine predators. *Nat. Commun.* 4, 1–9

879 Mayot, N., D’Ortenzio, F., Uitz, J., Gentili, B., Ras, J., Vellucci, V., Golbol, M., Antoine, D., Claustre,  
880 H., 2017. Influence of the Phytoplankton Community Structure on the Spring and Annual Primary  
881 Production in the Northwestern Mediterranean Sea, *J. Geophys. Res.*, 122, 9918–9936.  
882 doi:10.1002/2016JC012668

883 The MerMex Group, 2011. Marine ecosystems’ responses to climatic and anthropogenic forcings in the  
884 Mediterranean. *Progr. Oceanogr.*, 91, 97-166.

885 Migon, C., Heimbürger-Boavida, L.E., Dufour, A., Chiffoleau, J.F., Cossa, D., 2020. Temporal  
886 variability of dissolved trace metals at the DYFAMED time-series station, Northwestern  
887 Mediterranean. *Mar. Chem.*, 225, 103846.

888 Mille, T., Cresson, P., Chouvelon, T., Bustamante, P., Brach-Papa, C., Bruzac, S., Rozuel, E.,  
889 Bouchacha, M., 2018. Trace metal concentrations in the muscle of seven marine species: Comparison  
890 between the Gulf of Lions (North-West Mediterranean Sea) and the Bay of Biscay (North-East  
891 Atlantic Ocean). *Mar. Pollut. Bull.*, 135, 9-16.

892 Milligan, A.J., Harrison, P.J., 2000. Effects of non-steady-state iron limitation on nitrogen assimilatory  
893 enzymes in the marine diatom *Thalassiosira weissflogii* (Bacillariophyceae). J. Phycol., 36, 78-86.

894 Moffett, J. W., Brand, L. E., 1996. Production of strong, extracellular Cu chelators by marine  
895 cyanobacteria in response to Cu stress. Limnology and oceanography, 41, 388-395.

896 Morel, F.M.M., Milligan, A.J., Saito, M.A. 2003. Marine bioinorganic chemistry: The role of trace  
897 metals in the oceanic cycles of major nutrients. Treatise Geochem., 6, 113-143.

898 Morel, F.M.M., 2008. The co-evolution of phytoplankton and trace element cycles in the oceans.  
899 Geobiology, 6, 318-324.

900 Moynier, F., Vance, D., Fujii, T., Savage, P., 2017. The Isotope Geochemistry of Zinc and Copper. Rev.  
901 Mineral. Geochem., 82, 543-600.

902 Muller, F.L.L., Larsen, A., Stedmon, C.A., Sondergaard, M., 2005. Interactions between algal–bacterial  
903 populations and trace metals in fjord surface waters during a nutrient-stimulated summer bloom.  
904 Limnol. Oceanogr., 50, 1855-1871.

905 Nfon, E., Cousins, I.T., Jarvinen, O., Mukherjee, A.B., Verta, M., Broman, D., 2009. Trophodynamics  
906 of mercury and other trace elements in a pelagic food chain from the Baltic Sea. Sci. Total Environ.,  
907 407, 6267-6274.

908 Nriagu, J.O., Pacyna, J.M., 1988. Quantitative assessment of worldwide contamination of air, water and  
909 soils by trace metals. Nature, 333, 134-139.

910 Obiakor, M.O., Tighe, M., Pereg, L., Wilson, S.C., 2017. Bioaccumulation, trophodynamics and  
911 ecotoxicity of antimony in environmental freshwater food webs. Crit. Rev. Environ. Sci., 47, 2208-  
912 2258.

913 OECD, 2012. Test Guideline 305. Bioaccumulation in Fish: Aqueous and Dietary Exposure. Adopted 2  
914 October 2012.

915 Ohnemus, D., Lam, P.J., 2015. Cycling of lithogenic marine particles in the US GEOTRACES North  
916 Atlantic transect. Deep-Sea Res. II, 116, 283-302.

917 Ollivier, P., Radakovitch, O., Hamelin, B., 2011. Major and trace element partition and fluxes in the  
918 Rhône River. Chem. Geol., 285, 15-31.

919 Pacyna, J.M., Pacyna, E.G., 2001. An assessment of global and regional emissions of trace metals to the  
920 atmosphere from anthropogenic sources worldwide. *Environ. Rev.*, 9, 269-298.

921 Pasqueron de Fommervault, O., Migon, C., D'Ortenzio, F., Ribera d'Alcalà, Coppola, L., 2015.  
922 Temporal variability of nutrient concentrations in the northwestern Mediterranean Sea (DYFAMED  
923 time-series station). *Deep Sea Res. I*, 100, 1-12.

924 Peers, G., Quesnel, S.A., Price, N.M., 2005. Copper requirements for iron acquisition and growth of  
925 coastal and oceanic diatoms. *Limnol. Oceanogr.*, 50, 1149-1158.

926 Pempkowiak, J., Walkusz-Miotk, J., Beldowski, J., Walkusz, W., 2006. Heavy metals in zooplankton  
927 from the Southern Baltic. *Chemosphere*, 62, 1697-1708.

928 Pérez, S., Beiras, R., 2010. The mysid *Siriella armata* as a model organism in marine ecotoxicology:  
929 comparative acute toxicity sensitivity with *Daphnia magna*. *Ecotoxicol.*, 19, 196-206.

930 Pettine, M., 2000. Redox Processes of Chromium in Sea Water. In: Gianguzza, A., Pelizetti, E.,  
931 Sammartano, S. (Ed). *Chemical Processes in Marine Environments*. Environmental Science.  
932 Springer, Berlin.

933 Planquette, H., Sherrell, R.M., 2012. Sampling for particulate trace element determination using water  
934 sampling bottles: methodology and comparison to in situ pumps. *Limnol. Oceanogr. Methods*, 10,  
935 367-388.

936 Pujo-Pay, M., Conan, P., Oriol, L., Cornet-Barthaux, V., Falco, C., Ghiglione, J.-F., Goyet, C., Moutin,  
937 T., Prieur, L., 2011. Integrated survey of elemental stoichiometry (C, N, P) from the western to  
938 eastern Mediterranean Sea, *Biogeosciences*, 8, 883–899.

939 Quigg, A., Finkel, Z.V., Irwin, A.J., Rosenthal, Y., Ho, T.Y., Reinfelder, J.R., Schofield, O., Morel,  
940 F.M.M., Falkowski, P.G., 2003. The evolutionary inheritance of elemental stoichiometry in marine  
941 phytoplankton. *Nature*, 425, 291-294.

942 Radakovich, O., Roussiez, V., Ollivier, P., Ludwig, W., Grenz, C., Probst, J.L., 2008. Particulate heavy  
943 metals input from rivers and associated sedimentary deposits on the Gulf of Lions continental shelf.  
944 *Estuar. Coast. Shelf Sci.*, 77, 285-295.

945 Raimbault, P., Diaz, F., Pouvesle W., Boudjellal, B., 1999. Simultaneous determination of particulate  
946 organic carbon, nitrogen and phosphorus collected on filters, using a semiautomatic wet-oxidation  
947 method. *Mar. Ecol. Prog. Ser.*, 180, 289-295.

948 Rainbow, P.S., 2007. Trace metal bioaccumulation: models, metabolic availability and toxicity.  
949 *Environ. Int.*, 33, 576-582.

950 Ramírez-Romero, E., Molinero, J.C., Sommer, U., Salhi, N., Kefi- Daly Yahia, O., Daly Yahia, M.N.,  
951 2020. Phytoplankton size changes and diversity loss in the southwestern Mediterranean Sea in  
952 relation to long-term hydrographic variability. *Estuarine, Coastal and Shelf Science*, 235, 106574.

953 Rauch, J.N., 2010. Global spatial indexing of the human impact on Al, Cu, Fe and Zn mobilization.  
954 *Environ. Sci. Technol.*, 44, 5728-5734.

955 Redfield, A.C., 1958. The biological control of chemical factors in the environment. *Am. Sci.*, 46, 205-  
956 221.

957 Rentería-Cano, M.E., Sánchez-Velasco, L., Shumilin, E., Lavín, M.F., Gómez-Gutiérrez, J., 2011.  
958 Major and trace elements in zooplankton from the northern gulf of California during summer. *Biol.*  
959 *Trace Elem. Res.*, 142, 848–864

960 Roesijadi, G., Robinson, W.E., 1994. Metal regulation in aquatic animals: mechanisms of uptake,  
961 accumulation and release. *Aquat. Toxicol.* 102, 125-133.

962 Salhi, N., Zmerli Triki, H., Molinero, J.C., Laabir, M., Sehli, E., Bellaaj-Zouari, A., Daly Yahia, N.,  
963 Kefi-Daly Yahia, O., 2018. Seasonal variability of picophytoplankton under contrasting  
964 environments in northern Tunisian coasts, southwestern Mediterranean Sea. *Marine Pollution*  
965 *Bulletin*, 129, 866–874.

966 Sanganyado, E., Bi, R., Teta, C., Buruaem Moreira, L., Yu, X., Yajing, S., Dalu, T., Rajput, I.R., Liu,  
967 W., 2021. Toward an integrated framework for assessing micropollutants in marine mammals:  
968 challenges, progress, and opportunities. *Crit. Rev. Environ. Sci. Technol.* 51, 2824–2871

969 Schlesinger, W.H., Klein, E.M., Vengosh, A., 2017. Global biogeochemical cycle of vanadium. *Proc.*  
970 *Nat. Acad. Sci. U. S. A.*, 114, E11092-E11100.

971 Semeniuk, D.M., Maldonado, M.T., Jaccard., S.L., 2016. Chromium uptake and adsorption in marine  
972 phytoplankton – Implications for the marine chromium cycle. *Geochim. Cosmochim. Acta*, 184, 41-  
973 54

974 Sherrell, R.M., Boyle, E.A., 1988. Zinc, chromium, vanadium and iron in the Mediterranean Sea. *Deep*  
975 *Sea Res.*, 35, 1319-1334.

976 Srichandan, S., Panigraphy, R.C., Baliarsingh, S.K., Srinivasa, R.B., Premalata, P., Sahu, B.K., Sahu,  
977 K.C., 2016. Distribution of trace metals in surface seawater and zooplankton of the Bay of Bengal,  
978 off Rushikulya estuary, East Coast of India. *Mar. Pollut. Bul.*, 111, 468-475.

979 Sunda, W., 2012. Feedback interactions between trace metal nutrients and phytoplankton in the ocean.  
980 *Front. Microbiol.*, 3, 204.

981 Sunda, W., Huntsman, S.A., 1995. Regulation of copper concentration in the oceanic nitracline by  
982 phytoplankton uptake and regeneration cycles. *Limnol. Oceanogr.*, 40, 132-137.

983 Takano, S., Tanimizu, M., Hirata, T., Sohrin, Y., 2014. Isotopic constraints on biogeochemical cycling  
984 of copper in the ocean. *Nat. Com.*, 5, 5663.

985 Tanhua, T., Hainbucher, D., Schroeder, K., Cardin, V., Alvarez, M., Civitarese, G., 2013. The  
986 Mediterranean Sea system: a review and an introduction to the special issue. *Ocean Sci.*, 9, 789-803.

987 Takayanagi, K., Cossa, D., Martin, J.M., 1996. Antimony cycling in the western Mediterranean. *Mar.*  
988 *Chem.*, 54, 303-312.

989 Tedetti, M., Tronczynski, J., Carlotti, F., Pagano, M., Sammari, C., Bel Hassen, M., Ben Ismail, S.,  
990 Desboeufs, K., Poindron, C., Chifflet, S., Abdennadher, M., Amri, S., Bănarua, D., Ben Abdallah,  
991 L., Bhairy, N., Boudriga, I., Bourin, A., Brach-Papa, C., Briant, N., Cabrol, L., Chevalier, C.,  
992 Chouba, L., Coudray, S., Daly Yahia, M.N., de Garidel-Thoron T., Dufour, A., Dutay, J.-C.,  
993 Espinasse, B., Fierro, P., Fornier, M., Garcia, N., Giner, F., Guigue, C., Guilloux, L., Hamza, A.,  
994 Heimbürger-Boavida, L.-E., Jacquet, S., Knoery, J., Lajnef, R., Makhlouf Belkahia, N., Malengros,  
995 D., Martinot, P.L., Bosse, A., Mazur, J.-C., Meddeb, M., Misson, B., Pringault, O., Quéméneur, M.,  
996 Radakovitch, O., Raimbault, P., Ravel, C., Rossi, V., Rwawi, C., Sakka Hlaili, A., Tesán-Onrubia,  
997 J.A., Thomas, B., Thyssen, M., Zaaboub, N., Bellaaj-Zouari, A., Garnier, C., 2022. Contamination  
998 of planktonic food webs in the Mediterranean Sea: Setting the frame for the MERITE-

999 HIPPOCAMPE oceanographic cruise (spring 2019). Mar. Pollut. Bull., submitted to this special  
1000 issue.

1001 Tesán-Onrubia, J.A., Tedetti, M., Carlotti, F., Tenaille, M., Guilloux, L., Pagano, M., Lebreton, B.,  
1002 Guillou, G., Fierro-Gonzalez, P., Guigue, C., Chifflet, S., Garcia, T., Boudriga, I., Belhassen, M.,  
1003 Bellaaj-Zouari, A., Bănaru, D. Spatial variations of stable isotope ratios and biochemical content of  
1004 size-fractionated plankton in the Mediterranean Sea (MERITE-HIPPOCAMPE campaign). Mar.  
1005 Pollut. Bull., submitted to this special issue.

1006 Tessier, E., Garnier, C., Mullot, J.U., Lenoble, V., Arnaud, M., Raynaud, M., Mounier, S., 2011. Study  
1007 of the spatial and historical distribution of sediment inorganic contamination in the Toulon bay  
1008 (France). Mar. Pollut. Bull., 62, 2075-2086.

1009 Tlili, S., Ovaert, J., Souissi, A., Ouddane, B., Souissi, S., 2016. Acute toxicity, uptake and accumulation  
1010 kinetics of nickel in an invasive copepod species: *Pseudodiaptomus marinus*. Chemosphere, 144,  
1011 1729-1737.

1012 Twining, B.S., Baines, S.B., 2013. The trace metal composition of marine phytoplankton. Annu. Rev.  
1013 Mar. Sci., 5, 191-215.

1014 Twining, B.S., Fisher, N.S., 2004. Trophic transfer of trace metals from protozoa to mesozooplankton.  
1015 Limnol. Oceanogr., 49, 28-39.

1016 Turekian, K.K., 1977. The fate of metals in the ocean. Geochim. Cosmochim. Acta, 41, 1139-1144.

1017 UNEP/MAP-RAC-SPA, 2008. Impact of climate change on biodiversity in the Mediterranean Sea. In:  
1018 Perez T., RAC/SPA (Eds.), Tunis, 1-61.

1019 US EPA. 2007. Framework for Metals Risk Assessment. EPA-120-R-07-001. United States  
1020 Environmental Protection Agency, Washington DC.

1021 Uitz, J., Claustre, H., Morel, A., Hooker, S.B., 2006. Vertical distribution of phytoplankton communities  
1022 in open ocean: An assessment based on surface chlorophyll. J. Geophys. Res., 111, C08005.

1023 Uthus, E.O., 2003. Arsenic essentiality: a role affecting methionine metabolism. J. Trace Elem. Exp.  
1024 Med., 16, 345-355.

1025 Wang, W.X., 2002. Interactions of trace metals and different marine food chains. Mar. Ecol. Prog. Ser.,  
1026 243, 295-309.

- 1027 Warnau, M., Gómez-Batista, M., Alonso-Hernández, Carlos, Regoli, F., 2006. Arsenic: is it worth  
1028 monitoring in the Mediterranean Sea? In: CIESM Workshop Monographs n°31, 83-86.
- 1029 Whitfield, M., 2001. Interactions between phytoplankton and trace metals in the ocean. *Adv. Mar. Biol.*,  
1030 41, 1-128.
- 1031 Wrench, J., Fowler, S.W., Ünlü, M.Y., 1979. Arsenic metabolism in a marine food chain. *Mar. Pollut.*  
1032 *Bull.*, 10, 18-20.
- 1033 Wurl, O., Zimmer, L., Cutter, G.A., 2013. Arsenic and phosphorus biogeochemistry in the ocean:  
1034 Arsenic species as proxies for P-limitation. *Limnol. Oceanogr.*, 58, 729-740.
- 1035 Xu, Y., Feng, L., Jeffrey, P.D., Shi, Y.D., Morel, F.M.M., 2008. Structure and metal exchange in the  
1036 cadmium carbonic anhydrase of marine diatoms. *Nature*, 452, 56-61.



1037 **Table 1.** Variations of biotic metal (bM) concentrations in all fractions reported per element and per geographical areas. Statistical values (mean  $\pm$  standard  
 1038 deviation, min and max concentrations) were expressed in  $\mu\text{g/g}$ . The coefficient of variation (CV) was expressed in %. Data were compared with other values  
 1039 from suspended particulate matter and zooplankton collected in Mediterranean Sea.

<b>Biotic trace metals</b>	<b>As</b>	<b>Cd</b>	<b>Cr</b>	<b>Cu</b>	<b>Fe</b>	<b>Mn</b>	<b>Ni</b>	<b>Sb</b>	<b>V</b>	<b>Zn</b>
<i>North coastal zone (Marseilles-Toulon bays, 4 stations: St1, St2, St3, St4; n = 25)</i>										
<i>Mean (<math>\mu\text{g/g}</math>)</i>	6.7 $\pm$ 3.6	0.52 $\pm$ 0.44	7.9 $\pm$ 8.1	5.9 $\pm$ 3.9	212 $\pm$ 119	6.7 $\pm$ 4.6	1.4 $\pm$ 0.6	0.41 $\pm$ 0.27	8.4 $\pm$ 15	93 $\pm$ 63
<i>Min (<math>\mu\text{g/g}</math>)</i>	1.8	0.04	0.08	1.6	35	0.84	0.55	0.10	0.27	25
<i>Max (<math>\mu\text{g/g}</math>)</i>	14	1.7	26	17	527	20	2.7	1.0	49	261
<i>CV (%)</i>	54	84	102	66	56	69	45	66	183	68
<i>Offshore zone (Western Mediterranean Sea, 3 stations: St9, St10, St11; n = 18)</i>										
<i>Mean (<math>\mu\text{g/g}</math>)</i>	12.7 $\pm$ 13.1	0.83 $\pm$ 0.60	2.1 $\pm$ 3.0	6.9 $\pm$ 2.8	389 $\pm$ 258	5.3 $\pm$ 3.2	2.9 $\pm$ 1.3	4.9 $\pm$ 8.0	2.0 $\pm$ 1.3	139 $\pm$ 58
<i>Min (<math>\mu\text{g/g}</math>)</i>	0.60	0.10	0.27	1.6	50	1.5	0.78	0.01	0.48	41
<i>Max (<math>\mu\text{g/g}</math>)</i>	50	2.4	13	13	838	14	5.9	25	3.9	260
<i>CV (%)</i>	103	72	146	40	66	60	44	166	63	42
<i>South coastal zone (Gulf of Gabès, 3 stations: St15, St17, St19; n = 12)</i>										
<i>Mean (<math>\mu\text{g/g}</math>)</i>	2.4 $\pm$ 1.3	0.52 $\pm$ 0.25	4.0 $\pm$ 2.8	3.5 $\pm$ 2.3	209 $\pm$ 146	11 $\pm$ 17	1.9 $\pm$ 1.4	4.7 $\pm$ 4.4	4.0 $\pm$ 6.1	75 $\pm$ 44
<i>Min (<math>\mu\text{g/g}</math>)</i>	0.14	0.03	0.39	0.4	13	0.02	0.08	0.07	0.08	5.0
<i>Max (<math>\mu\text{g/g}</math>)</i>	4.6	0.84	9.3	7.0	523	55	5.0	13	19	133
<i>CV (%)</i>	52	48	71	64	70	159	70	94	154	59
<i>Suspended particulate matter at the deep chlorophyll maximum (spring and summer 2010), Gulf of Lions<sup>1</sup></i>										
<i>Mean (<math>\mu\text{g/g}</math>)</i>	-	0.35 $\pm$ 0.19	-	14 $\pm$ 15	-	-	16 $\pm$ 25	-	-	152 $\pm$
<i>Min (<math>\mu\text{g/g}</math>)</i>	-	0.14	-	3.3	-	-	1.8	-	-	41
<i>Max (<math>\mu\text{g/g}</math>)</i>	-	0.58	-	20	-	-	66	-	-	439
<i>Zooplankton (Spring 2014), Offshore Italian coasts<sup>2</sup></i>										
<i>5-50 m depth (<math>\mu\text{g/g}</math>)</i>	0.46	0.08	7.25	4.64	539	5.55	5.48	0.48	0.89	132
<i>50-100 m depth (<math>\mu\text{g/g}</math>)</i>	0.65	0.16	0.87	3.72	1742	8.82	2.04	0.59	1.18	80

1040 <sup>1</sup>Choulevon et al., 2019 ; <sup>2</sup>Battuello et al., 2016

1041 **Table 2:** Mean bM/POP ratio  $\pm$  standard deviation (mmol/mol) in planktonic food webs per element and geographical areas. Mean bM/POP ratios were  
1042 calculated including all fractions (n = 25 in the northern coastal zone; n = 18 in the offshore zone; n = 12 in the southern coastal zone).

	<b>Northern coastal zone</b>	<b>Offshore zone</b>	<b>Southern coastal zone</b>
<i>As</i>	1.11 $\pm$ 0.74	1.06 $\pm$ 0.76	0.39 $\pm$ 0.11
<i>Cd</i>	0.04 $\pm$ 0.02	0.06 $\pm$ 0.05	0.06 $\pm$ 0.03
<i>Cr</i>	1.37 $\pm$ 1.36	0.33 $\pm$ 0.39	0.91 $\pm$ 0.26
<i>Cu</i>	0.89 $\pm$ 0.34	0.85 $\pm$ 0.37	0.65 $\pm$ 0.15
<i>Fe</i>	38.0 $\pm$ 11.0	45.3 $\pm$ 23.0	40.4 $\pm$ 10.1
<i>Mn</i>	1.18 $\pm$ 0.51	0.62 $\pm$ 0.13	3.36 $\pm$ 5.1
<i>Ni</i>	0.24 $\pm$ 0.04	0.35 $\pm$ 0.07	0.37 $\pm$ 0.12
<i>Sb</i>	0.03 $\pm$ 0.01	0.17 $\pm$ 0.31	0.38 $\pm$ 0.54
<i>V</i>	3.35 $\pm$ 6.28	0.27 $\pm$ 0.14	1.39 $\pm$ 2.04
<i>Zn</i>	13.08 $\pm$ 5.00	13.98 $\pm$ 5.22	12.47 $\pm$ 3.95

1043

**Table 3:** Trophic magnification factor (TMF) of essential (Cd, Cu, Fe, Mn, Ni, V, Zn) and non-essential (As, Cr, Sb) elements along the North-South Mediterranean transect. TMF values were calculated from the regression line between log-transformed bM and trophic level (see Appendix 2 for supplementary information), per geographic area and element. Statistical measures ( $r^2$ ) indicated how the model fit with values.

	Essential elements						Non-essential elements			
	Cd	Cu	Fe	Mn	Ni	V	Zn	As	Cr	Sb
<i>Northern coastal zone (n = 25)</i>										
TMF	3.9	2.2	1.4	2.7	1.6	2.2*	2.6	1.1	2.1	3.1
$r^2$	0.26	0.34	0.22	0.45	0.20	0.49	0.40	0.30	0.38	0.37
<i>Offshore zone (n = 18)</i>										
TMF	1.1	1.1	2.0	2.0	0.9	0.9	1.2	1.3	0.8	1.3
$r^2$	0.12	0.3	0.59	0.86	0.20	0.30	0.74	0.23	0.23	0.17
<i>Southern coastal zone (n = 12)</i>										
TMF	7.5	6.6	9.6	1.2	3.8	1.3	4.7	3.9	5.8	5.7
$r^2$	0.71	0.47	0.45	0.24	0.36	0.10	0.63	0.50	0.39	0.11

\* TMF (n = 20)

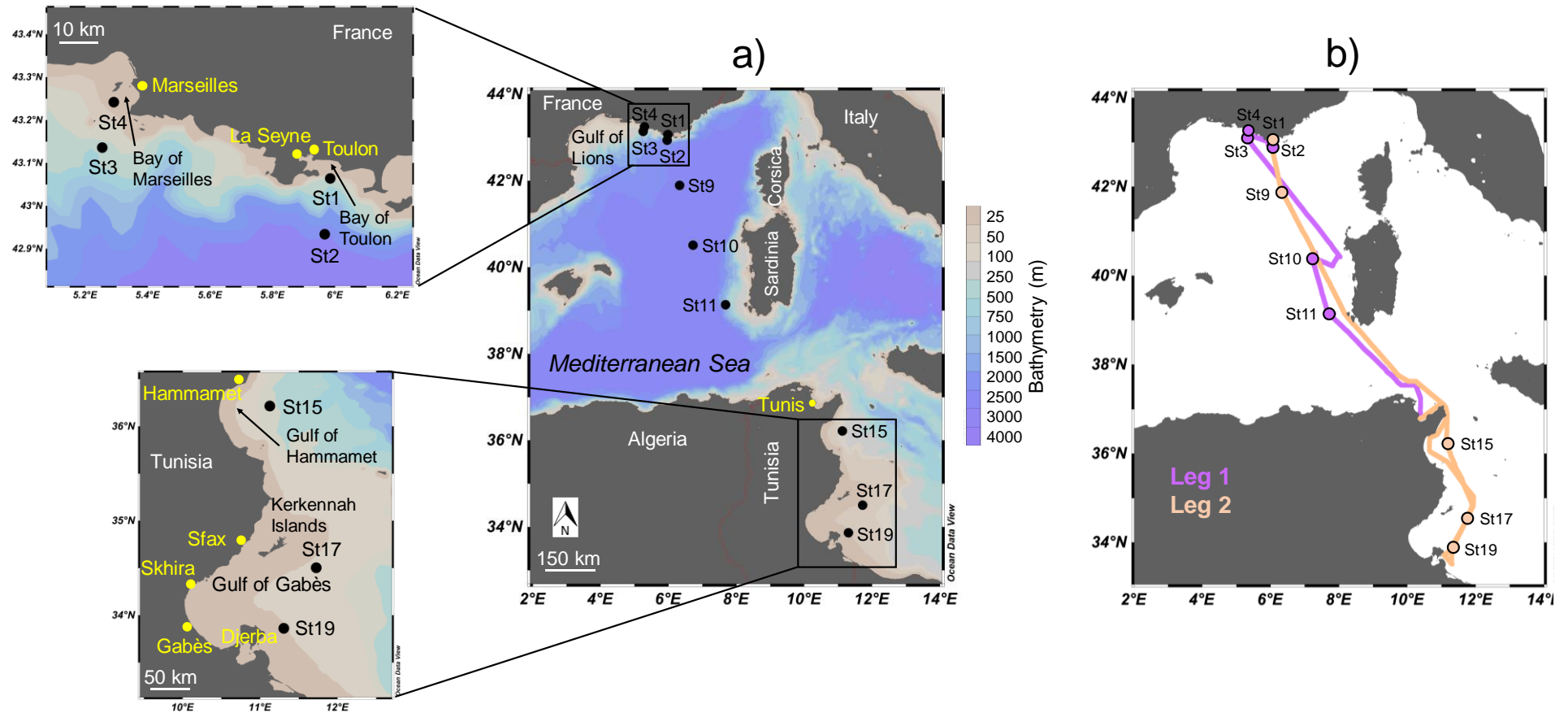
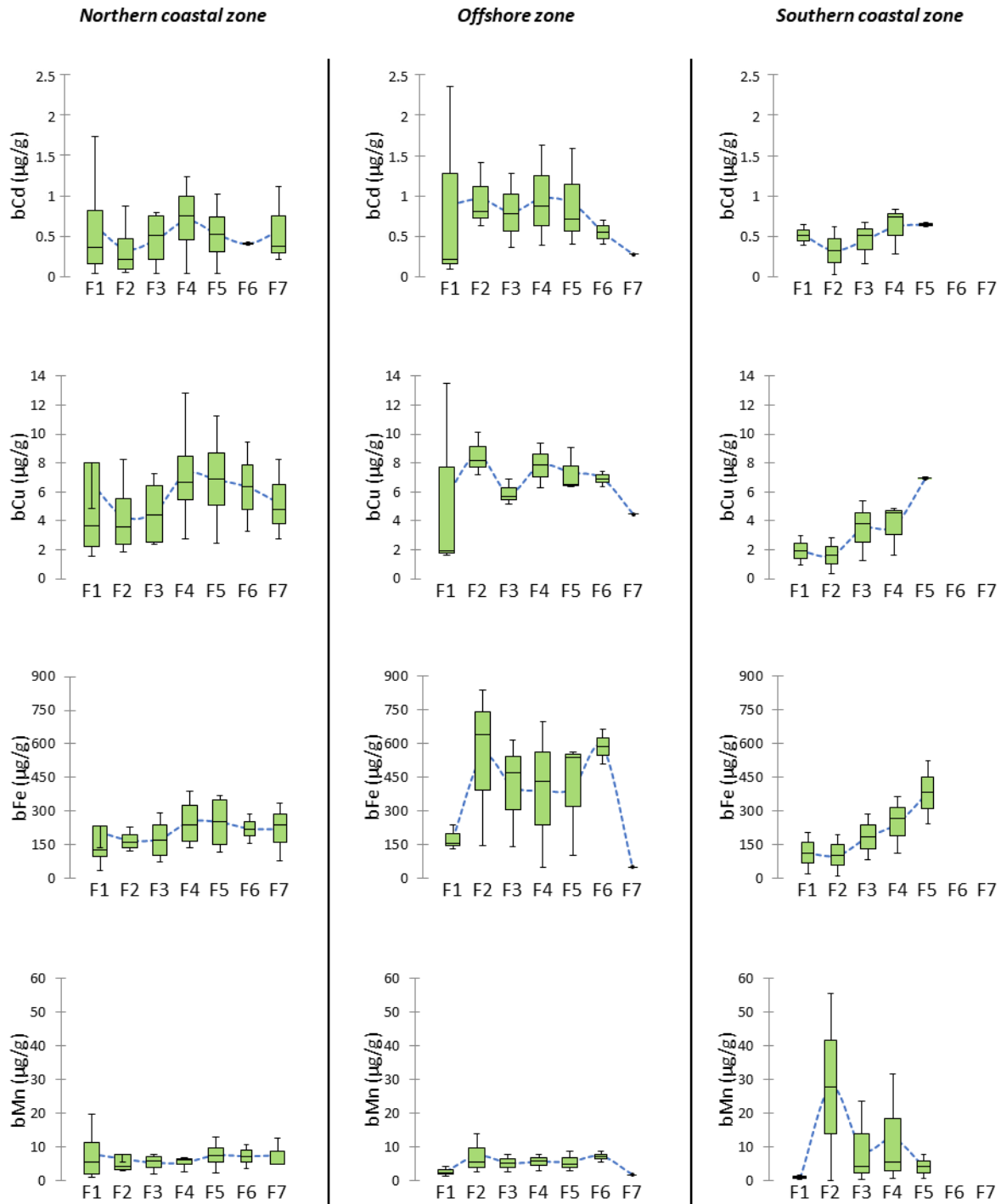


**Figure 1.** a) Location of the sampling stations in the Mediterranean Sea. b) Details of the MERITE-HIPPOCAMPE campaign tracks: Leg 1 (from La Seyne-sur-Mer to Tunis) with 5 sampling stations (St2, St4, St3, St10 and St11 in chronological order); Leg 2 (from Tunis to the Gulf of Gabès to La Seyne-sur-Mer) with 5 sampling stations (St15, St17, St19, St9 and St1 in chronological order).

ESSENTIAL ELEMENTS

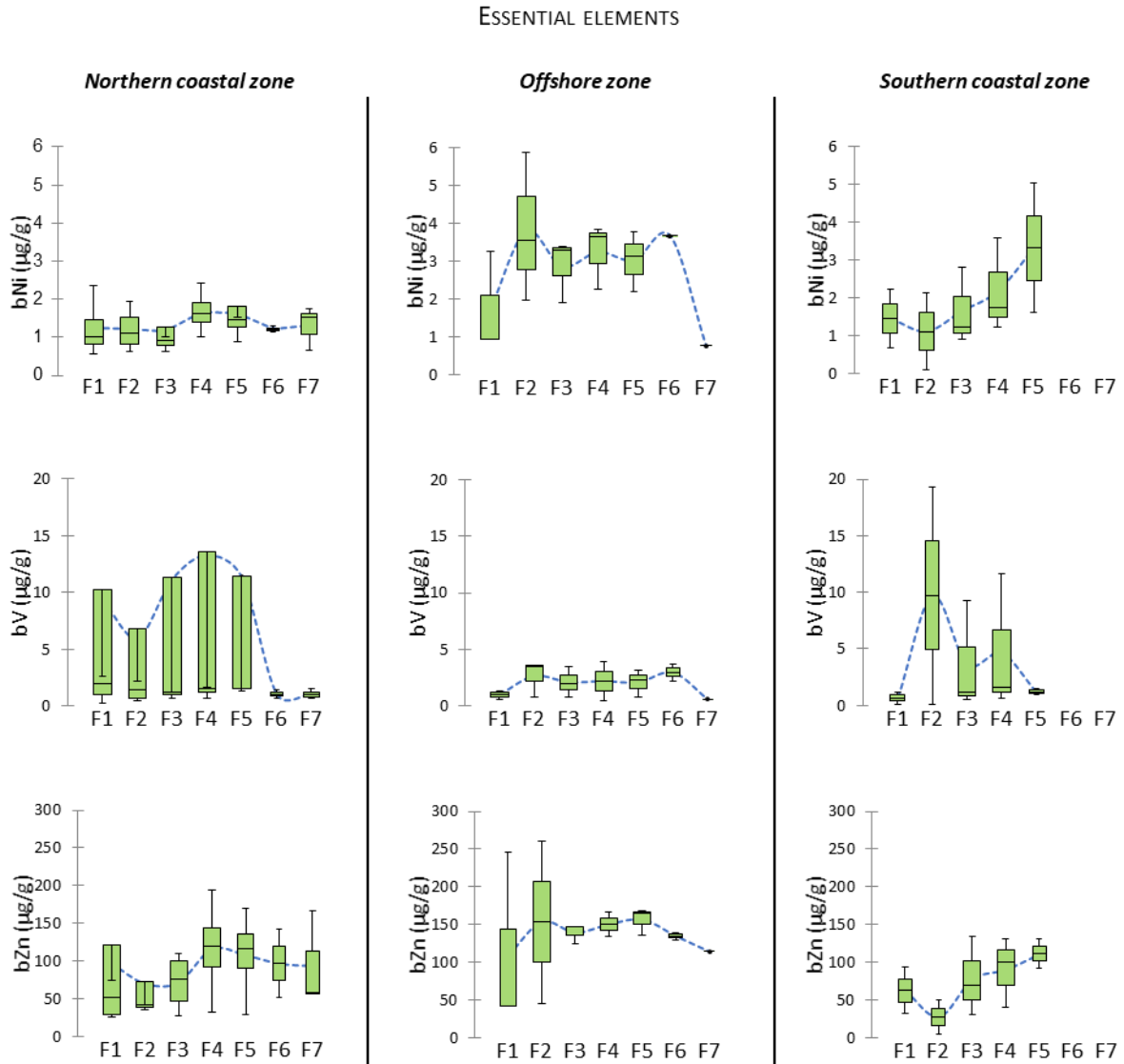


1

2 **Figure 2.** Trophic distribution of 7 essential elements (Cd, Cu, Fe, Mn, Ni, V, Zn) in 3 geographical  
 3 areas along the North-South Mediterranean transect. The boxplots represent the variations in bCd, bCu,  
 4 bFe, bMn, bNi, bV and bZn concentrations ( $\mu\text{g/g}$ ) in the northern coastal zone (4 stations, St1-4),  
 5 offshore zone (3 stations, St9-11) and southern zone (3 stations, St15, St17, St19) and include the 7  
 6 particle size-fraction classes (F1: 0.8–3  $\mu\text{m}$ ; F2: 3–20  $\mu\text{m}$ ; F3: 60–200  $\mu\text{m}$ ; F4: 200–500  $\mu\text{m}$ ; F5: 500–

7 1000  $\mu\text{m}$ ; F6: 1000–2000  $\mu\text{m}$ ; F7 > 2000  $\mu\text{m}$ ). Boxplots show the first quartile (25%), median, and third  
 8 quartile (75%). The dashed blue line plots the median bM concentrations. Box plots were created using  
 9 XLstat software package version 2019.1.1 (Addinsoft 2020, Boston, USA, <https://www.xlstat.com>).

10

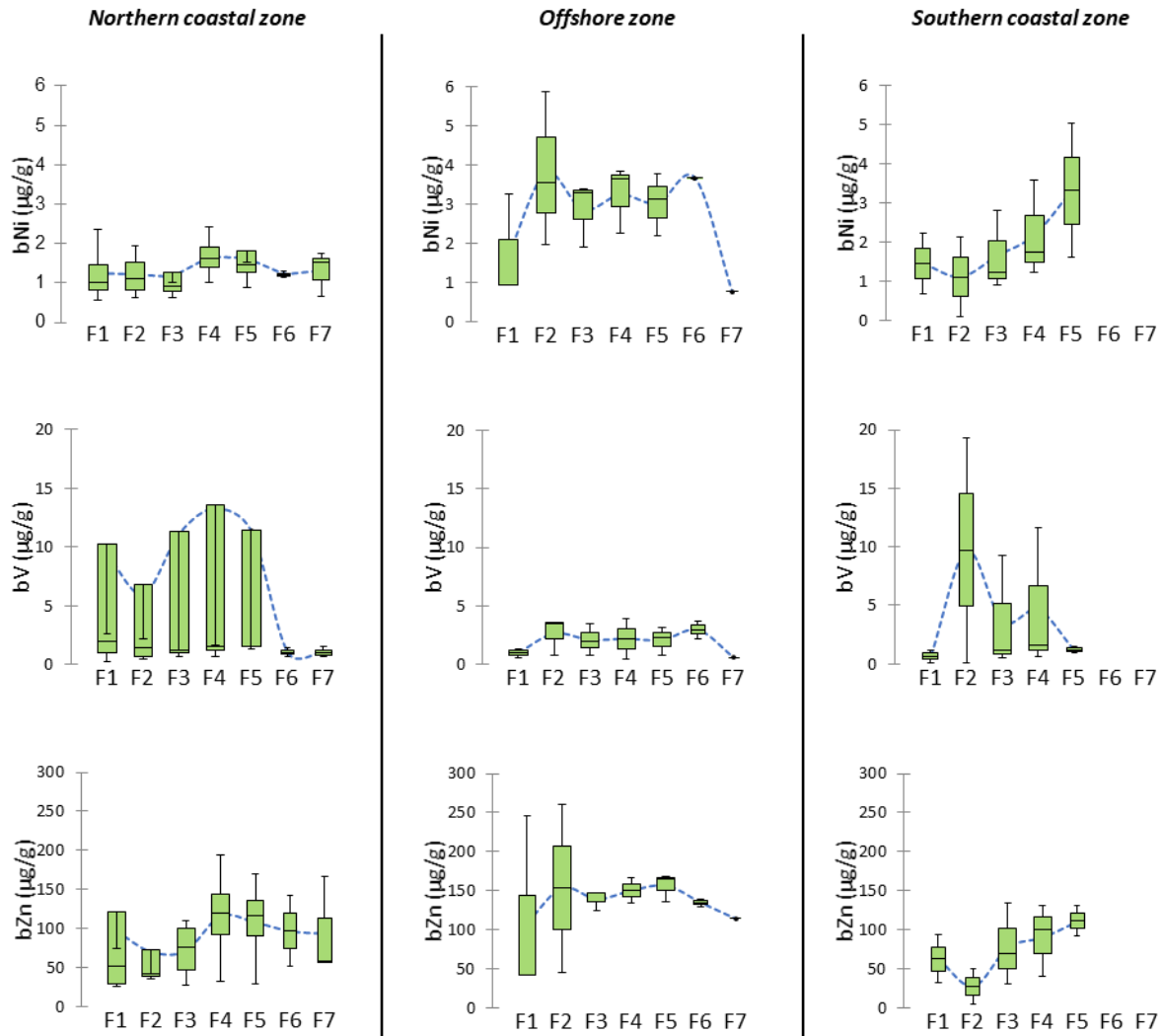


11

12

Figure 2 (continue)

ESSENTIAL ELEMENTS



13

14 **Figure 3.** Trophic distribution of 3 non-essential elements (As, Cr, Sb) in 3 geographical areas along  
 15 the North-South Mediterranean transect. The boxplots represent the variations in  $bAs$ ,  $bCr$  and  $bSb$   
 16 concentrations ( $\mu\text{g/g}$ ) in the northern coastal zone (4 stations, St1-4), offshore zone (3 stations, St9-11)  
 17 and southern zone (3 stations, St15, St17, St19) and include the 7 particle size-fraction classes (F1: 0.8–  
 18 3  $\mu\text{m}$ ; F2: 3–20  $\mu\text{m}$ ; F3: 60–200  $\mu\text{m}$ ; F4: 200–500  $\mu\text{m}$ ; F5: 500–1000  $\mu\text{m}$ ; F6: 1000–2000  $\mu\text{m}$ ; F7 >  
 19 2000  $\mu\text{m}$ ). Boxplots show the first quartile (25%), median, and third quartile (75%). The dashed blue  
 20 line plots the median  $bM$  concentrations. Box plots were created using Xlstat software package version  
 21 2019.1.1 (Addinsoft 2020, Boston, USA, <https://www.xlstat.com>).

22